May 2016

Characterization of DOM and Its Interactions with Invasive Quagga Mussels in Lake Michigan

Stephen DeVilbiss
University of Wisconsin-Milwaukee

CHARACTERIZATION OF DISSOLVED ORGANIC MATTER AND ITS INTERACTIONS WITH INVASIVE QUAGGA MUSSELS IN LAKE MICHIGAN

by

Stephen DeVilbiss

A Thesis Submitted in

Partial Fulfillment of the

Requirements for the Degree of

Master of Science

in Freshwater Sciences and Technology

at

The University of Wisconsin-Milwaukee

May 2016

ABSTRACT

CHARACTERIZATION OF DISSOLVED ORGANIC MATTER AND ITS INTERACTIONS WITH INVASIVE QUAGGA MUSSELS IN LAKE MICHIGAN

By

Stephen DeVilbiss

The University of Wisconsin-Milwaukee, 2016
Under the Supervision of Professor Laodong Guo

Green Bay is the largest freshwater estuary in the Laurentian Great Lakes and receives disproportional terrestrial inputs. While seasonal hypoxia and the formation of "dead zones" in Green Bay have received increasing attention, there are no systematic studies on the dynamics of dissolved organic matter (DOM) and its linkage to the development of hypoxia. During summer 2014, bulk dissolved organic carbon (DOC) analysis, UV-vis spectroscopy, and fluorescence excitation-emission matrices (EEMs) coupled with PARAFAC analysis were used to quantify the abundance, composition and source of DOM and their spatiotemporal variations in Green Bay, Lake Michigan. Concentrations of DOC ranged from 202 to 571 μM-C (average = 361±73 μM-C) in June and from 279 to 610 μM-C (average = 349±64 μM-C) in August. In both months, absorption coefficient at 254 nm (a_{254}) was strongly correlated to bulk DOC and was most abundant in the Fox River, attesting to a dominant terrestrial input. Non-chromophoric DOC comprised, on average, ~32% of the bulk DOC in June with higher terrestrial DOM and ~47% in August with higher aquagenic DOM, indicating that autochthonous and more degraded DOM is of lower optical activity. PARAFAC modeling on EEM data resulted in four major fluorescent DOM components, including two terrestrial humic-like, one aquagenic humic-like, and one protein-like component. Variations in the abundance of DOM components further supported

changes in DOM sources. Mixing behavior of DOM components also indicated that while bulk DOM behaved quasi-conservatively, significant compositional changes occurred during transport from the Fox River to the open bay.

Quagga mussel infestation is another issue in the Great Lakes that has caused significant changes in food web structure and ecological function over the past decade. Nevertheless, linkages between invasive species and dynamics of carbon and nutrients in Lake Michigan are less clear. We report here yields of dissolved organic matter (DOM) and nutrients from quagga mussels as well as chemical composition and size spectra of excreted DOM. Clearance rates of different sized microparticles indicate that quagga mussel ctenidial fibers can efficiently retain DOM as small as 0.5 μm. Smaller mussels have higher DOM excretion rates (0.076±0.004 μmol-C $mgDW^{-1}$ d^{-1}) compared to larger mussels (0.012±0.0002 μmol-C $mgDW^{-1}$ d^{-1}). Nitrogen excretion rate was up to 0.24±0.01 μmol-N $mgDW^{-1}$ d^{-1}, 3 times higher than dissolved organic carbon (DOC), while inorganic phosphorus excretion was only 0.0076±0.0030 μmol-P $mgDW^{-1}$ d^{-1}. Excreted DOM was mostly chromophoric and high-molecular-weight in nature with a colloidal size spectrum centered at 1-5 kDa, had a low C/N but higher N/P ratio, and was comprised of up to 78% carbohydrates with high abundance of structural polysaccharides. Fluorescence EEMs and PARAFAC analysis identified two major fluorescent DOM components: a tryptophan-like and a UVC humic-like, suggesting that excreted DOM could be potentially labile. Compared with field measurements, only ~12% of organic matter consumed by quagga mussels is excreted/egested, and the vast majority is likely respired as CO_2, potentially contributing to its supersaturation in the water column and changes in carbon dynamics in Lake Michigan after the colonization of invasive quagga mussel.

TABLE OF CONTENTS

LIST OF FIGURES

LIST OF TABLES

ACKNOWLEDGEMENTS

I sincerely thank my advisor Dr. Laodong Guo for his unwavering support and guidance. I also thank my advisory committee members Drs. Val Klump and Harvey Bootsma for their suggestions and and edits. I owe much thanks to the members of the Guo Lab, specifically Drs. Zhengzhen Zuo and Peng Lin, who's advice and assistance in laboratory and statistical analyses was tremendously beneficial.

This thesis research was supported in part by NOAA Wisconsin Sea Grant (R/HCE-16), NSF-MRI (#1233192), and the University of Wisconsin-Milwaukee (RGI and startup funds). Funding for sampling cruises to Green Bay/Lake Michigan was provided by NOAA Wisconsin Sea Grant (R/HCE-12 to JVK), the NOAA CSCOR Coastal Hypoxia Research Program (Grant NA10NOS4780139 to JVK), and the Michigan Water Center.

1. Introduction

1.1 The role and sources of dissolved organic matter in natural aquatic systems

Dissolved organic carbon (DOC) is the largest reserviour of active organic carbon in aquatic systems and consists of a heterogeneous mixture of aromatic and aliphatic reduced carbon compounds with associated functional groups (Guo et al. 1995; Leenheer and Croué 2003). Many natural processes are influenced by the presence of natural dissolved organic matter (DOM) including the cycling of trace metals and toxicants, biochemical oxygen demand (BOD), attenuation of photosynthetically active radiation (PAR), and toxicity of elements (e.g. heavy metals) and manufactured compounds to biological organisms making it important for aquatic ecosystem functions (Honeyman and Santchi, 1992; Sondergaard et al. 1995; Guo and Hunt 2001; Siegel and Michaels 1996). However, as a result of its heterogenous nature and diverse behavior in aquatic systems, DOC remains the least understood pool of organic carbon.

Dissolved organic matter originates from both allochthonous and autochthonous sources. Allochthonous DOM has numerous sources including terrestrial plant detritus, mineral soils, resuspended river sediments, riverine plankton exudates, as well as DOM from adjacent wetlands and marshes (Bauer and Bianchi 2011). Riverine systems are a major link between the geosphere and hydrosphere transporting terrestrially derived DOM to estuaries and open water systems subsequently affecting the abundance and composition of DOM (Guo et al. 2007; Bauer and Bianchi 2011). Conversely, autochthonous DOM is produced mainly by processes from the lower trophic groups including primary producers, bacteria, viruses, and grazers. Specfic pathways that release DOM from intact cells include sloppy feeding by grazers, viral lysis,

excretion of metabolites, and exudation of excracellular compounds (Coble 2007; Møller et al. 2003; Møller 2005; Rochelle-Newall and Fisher 2002).

1.2 Behavior of naturally occuring dissolved organic matter

Dissolved organic carbon displays diverse behaviors in aquatic systems and can be affected by a variety of factors. It was long thought that low molecular weight (LWM) DOM, which comprises between 65-80% of DOM in the global oceans, was rapidly remineralized while high molecular weight (HMW) DOM was biologically refractory (Benner et al. 1992; Kepkay et al. 1993). However, Amon and Benner (1994) found that bacterial growth and respiration in the presence of HMW DOM were three to six times greater than in the presence of LWM DOM indicating the majority of DOM in the global oceans may be biologically refractory and previous conceptions of HMW DOM were incorrect. Chemical composition also greatly affects the behavior of DOM in aquatic systems. Compounds such as free amino acids (FAA), sugars, carboxylic acids, and fatty acids have been shown to be biologically labile and readily taken up and remineralized by aquatic organisms (Thomas 1997; Baines et al. 2005; Crawford et al. 2015). Other compounds, including humic substances as well as FAA are highly photochemically labile and readily oxidize to form more labile DOM and dissolved inorganic carbon (DIC), making them not only important to aquatic carbon cycling, but also to the global carbon cycle as well (Kieber et al. 1989; Kieber et al. 1997). These properties of DOM are important factors that dictate the mixing behavior of DOM during river – open water mixing.

The behavior of organic matter during river – open water mixing is an important factor influencing the role of riverine DOM in aquatic ecosystem processes. Mixing plots, in which specific conductivity is used as a mixing index to generate a theorhetical mixing line, are often

used to assess the reactivity of constintuents at river-open water interfaces (Loder and Reichard 1981). When constituents plotted against specific conductivity fall on the theorhetical mixing line, they are classified as non-reactive and conservative. However, when points deviate from the mixing line, they are considered reactive and non-conservative either by means of addition or removal (Stedmon and Markager 2003). Addition processes may include *in situ* production or resuspension while removal processes consist of flocculation, sedimentation, and degradation to DIC (Uher et al. 2001).

Terrestrial organic matter (TOM) is comprised largely of recalcitrant, nitrogen-free macromolecules consisting largely of lignings and tannins (De Leeuw and Largeau 1993). It would therefore be logical to assume that TOM would behave conservatively during mixing being effected primary by dilution with open waters. However, despite resistance to microbial degradation, TOM does not comprise a significant fraction of oceanic DOM suggesting substantial removal during transport to open waters (Hedges and Keil 1995). Data suggests that at least 50% of TOM must be remineralized to CO_2, H_2O, and nutrients in order to be in accordance with global mass balances (Hedges et al. 1997). On the other hand, *in situ* produced DOM is highly reactive, turning over rapidly in the water column contributing to both addition and removal of DOM (Wakeham and Lee 1993). Markager et al. (2011) hypothsized that in systems with high inorganic nutrient loading such as the Horsens Fjord in Denmark or Green Bay, Lake Michigan, substantial assimilation of nutrients will result in the addition of autochthonous DOM. This was supported by their results indicating a net addition of DOM during the productive season and net removal during the winter.

1.3 Degradation pathways of natural dissolved organic matter

Degradation pathways of DOM are important processes influencing not only the mixing behavior of DOM, but the behavior of DOM in open water systems as well as the global carbon cycle . Both photochemical and biological processes impact the degradation of DOM in natural waters (Miller and Moran 1997). Biological degradation, specifically heterotrophic oxidation, has been shown to consume considerable dissolved oxygen (DO) in aquatic systems (Amon and Benner 1996; Amon and Benner 1996). Bacterial remineralization of DOM has even been linked to the establishement of the hypoxic "dead zone" in the Golf of Mexico, and similar trends have been observed for decades in Green Bay, Lake Michigan (Benner et al. 1992; Klump et al. 2009).

The fraction of DOM that participate in photochemical reactions absorb light over a broad range of UV and visible wavelengths and are referred to as chromophoric DOM (CDOM). Photochemical processes have been shown to either directly or indirectly effect numerous processes including underwater optical fields, trace element and contaminant distributions and cycling, as well as biological processes (Kieber et al. 1989; Siegel and Michaels 1996). For example, Kieber et al. (1989) showed that refractory, deep water DOM (>3000m) with a ^{14}C age of over 6000 years underwent photochemical degradation to pyruvate, a biologically labile organic compound. Other studies have shown the importance of photchemical degradation of DOM to the speciation, toxicity and fate of mercury and the cycling of trace elements like iron (Ravichandran 2004; Voelker et al. 1997).

Degradation of DOM can also produce greenhouse gases including CO_2 and CH_4. Therefore, the fate of DOM in natural waters impacts atmospheric greenhouse gas concentrations providing a direct link to the global carbon cycle and climate change (McGuire and Anderson 2009). For example, arctic warming has resulted in the mobilization of massive carbon stores in permafrost (Guo et al. 2007; Vonk et al. 2012). It was widely accepted, based on late summer

mixing studies, that permafrost derived DOC was highly refractory in nature and participated minimally in arctic biogeochemical cycling. However, more recent studies have showed signficant seasonal variations in the lability of this DOC source and indicate up to 40% removal of DOC during spring ice melt (Holmes et al. 2008). This has implications ranging from a positive feedback loop resulting from the increased greenhouse gas emmissions from DOC decomposition to stimulating primary production due concurrent remineralization of nutrients which would sequester CO_2 (Holmes et al. 2008).

2. Part I: Abundance, distributions, and variations in bulk and chromophoric DOM in Green Bay, Lake Michigan

2.1 Background

Freshwater bays and estuaries comprise some of the most biologically productive, yet anthropogenically stressed ecosystems in the Laurentian Great Lakes (Smith et al. 1988; Herdendorf 1990). Terrestrial inputs of nutrients and organic carbon are major components driving estuary biogeochemical cycling and have implications ranging from degraded ecosystem health to food web perturbations (Klump et al. 1997). Southern Green Bay has historically been classified as a hypereutrophic system as a result of high nutrient and organic carbon loading from the Lower Fox River, which drains some of the most intensely farmed land in Wisconsin (Ankley et al. 1992; Smith et al. 1988). Despite decades of nutrient regulation, Green Bay has continued to experience reeutrophication, recurring bouts of hypoxic conditions, and the formation of dead zones over the past years (Klump et al. 2009; Egen 2014).

Carbon dynamics can be closely related to dissolved oxygen (DO) and the development of hypoxia (Bianchi et al. 2010), as photochemical and heterotrophic oxidation of dissolved organic

matter (DOM) consumes DO in both surface and bottom waters (Diaz and Rosenberg 2008; Green et al. 2006). Additionally, DOM plays an important role in the fate and transport of many organic contaminants and heavy metals (McCarthy and Zachara 1989; Santschi et al., 1997). Therefore, knowledge of sources, abundance, chemical composition, and cycling pathways of DOM is important to better understanding of the overall ecosystem health in aquatic environments. There have been several studies on dissolved and particulate organic matter in Green Bay since the 1980s (Eadie et al. 1992; Achman 1993; O'loughlin and Chin 2009). However, the Green Bay ecosystem and Lake Michigan as a whole have experienced significant ecological and environmental change over the last two decades including increasing anthropogenic influence, the introduction of invasive species (Qualls et al. 2007; De Stasio et al. 2014), and increases in the extent of hypoxia (Egen 2014). Baseline data on the abundance, distribution, and composition of DOM in Green Bay are still lacking, but are indispensable for trend analysis and understanding the response of carbon dynamics to climate and environmental changes, especially the formation of hypoxia.

Dissolved organic matter is a heterogeneous mixture of reduced carbon compounds and comprises the largest pool of active organic matter in aquatic environments (Leenheer and Croué 2003; Guo et al. 2003). Aquatic systems receive DOM inputs from allochthonous and autochthonous sources such as riverine discharge and *in situ* production, respectively (Bauer and Bianchi 2011). Chromophoric dissolved organic matter (CDOM) is operationally defined as the fraction of bulk DOM that absorbs light over a broad range of visible and UV wavelengths (Coble 2007; Rochelle-Newall and Fisher 2002; Zhang et al. 2009). As such, CDOM plays many important roles in aquatic systems such as influencing biological production by regulating the penetration of photosynthetically active radiation, protecting organisms from UV radiation, and

contributing to the organic carbon cycle due to high photoreactivity (Belzile et al. 2002; Williamson et al. 1999). In addition to providing many important roles in aquatic systems, CDOM is also useful in tracing riverine inputs and biogeochemical cycling of DOM (Helms et al. 2008; Matsuoka et al. 2012). A sub-fraction of CDOM with fluorescent properties (fluorescent-DOM, or FDOM) has received increasing interest in recent years due to its usefulness as a proxy for the bulk DOC pool (Chen et al., 2003; Cory and McKnight, 2011). Fluorescence excitation-emission matrices (EEMs) combined with parallel factor analysis (PARAFAC) have been successfully used to identify allochthonous and autochthonous fluorescent DOM components in a diverse range of natural environments (Stedmon and Markager 2005; Wang et al. 2007; Chari et al. 2012; Xu et al. 2013). So far, there are no systematical studies on bulk DOC and chromophoric DOM in Green Bay using fluorescence EEMs coupled with PARAFAC modeling to track changes in DOM composition across the trophic gradient along the terrestrial-aquatic continuum in Green Bay.

2.2 Purpose of Study

The objectives of this study were to 1) examine the abundance, composition, spatial distribution, and temporal variation of DOC, CDOM, and FDOM in Green Bay; 2) evaluate the relative importance of non-chromophoric DOM and allochthonous and autochthonous DOM sources in different sampling months; 3) identify cycling processes and transformation pathways of DOM in the water column under different thermal stratification conditions and the linkage between DOM dynamics and hypoxic conditions; and 4) establish baseline data for trend analysis and to provide new insights into better understanding the impact of organic carbon loading to the health of Green Bay.

2.3 Methods

2.3.1 Study Site

Green Bay, located in northwestern Lake Michigan, is the largest freshwater estuary in the Laurentian Great Lakes (Fig. 1). The average depth of the bay is 20 m, ranging from ~3 m in the far southern end to 53 m in the north. Extending ~190 km from south to north and ~22 km from west to east, Green Bay has a volume of ~67 km^3. Green Bay's watershed drains about 40,000 km^2, which encompasses almost half of the drainage basin of Lake Michigan and resultantly is highly impacted by surrounding landscapes (Harris and Christie 1987; Klump et al. 1997). Of the 11 rivers and streams that drain into Green Bay, the Fox River is the largest input with a mean discharge of 118 $m^3 s^{-1}$ (Mortimer 1978). The Lower Fox River watershed is 50.2% agriculture, 34.6% urban, 14.7% natural forests and wetlands, and the remaining 0.6% under construction (WDNR, 2012). Additionally, the lower Fox River used to contain highest density of pulp and paper mills in the world resulting in large amounts of nutrients and contaminants being flushed into the southern portion of the bay (Harris and Christie 1987), consequently causing high productivity, eutrophic conditions and the formation of dead zones, especially in southern Green Bay (Valenta, 2013; Lin et al., 2016).

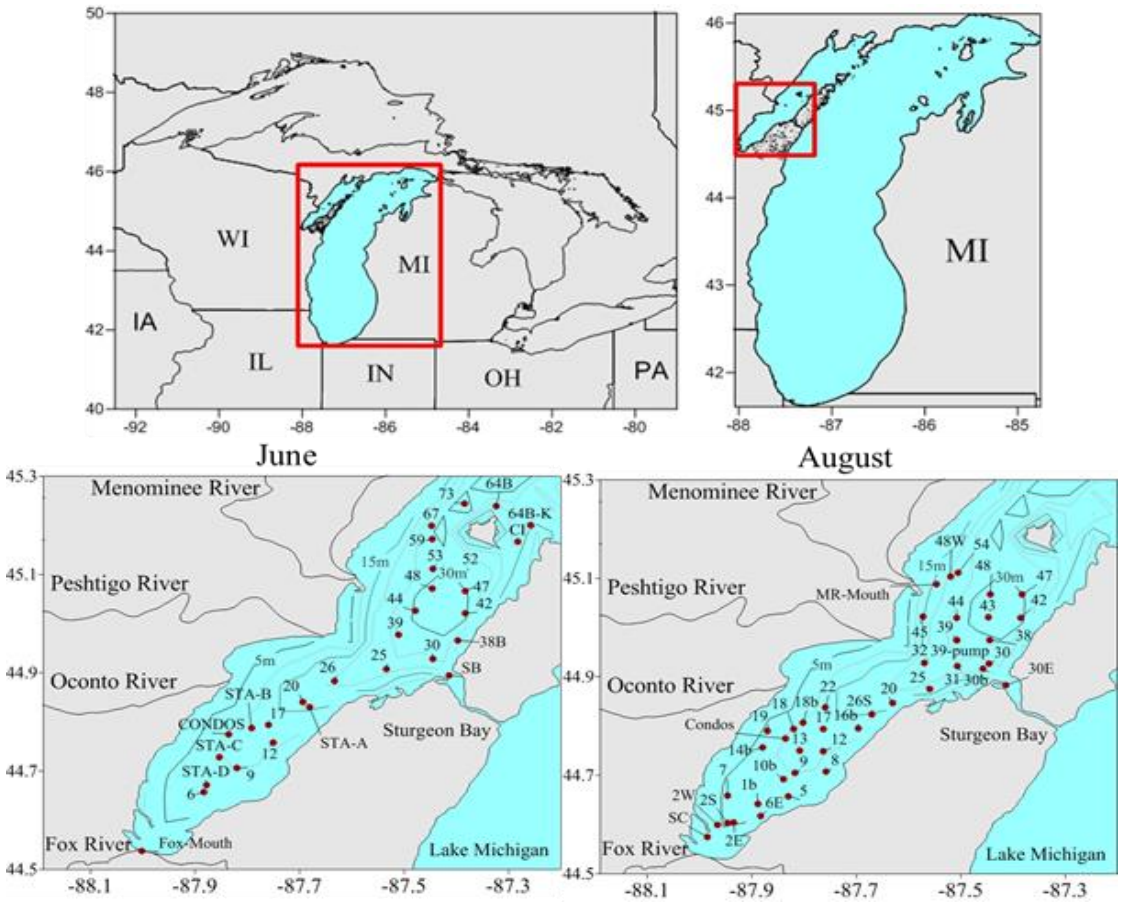

Figure 1: A map of the study area and sample locations in Green Bay, Lake Michigan in June and August 2014.

2.3.2 Field Sampling

Water samples were collected from Green Bay on board the RV Neeskay on the 4th and 5th of June 2014 and on the 24th, 25th, and 26th of August 2014 at 30 and 43 sampling locations, respectively (Fig. 1). Surface and depth water samples were taken with a submersible pump and stored in acid washed, triple-rinsed, 2 L HPDE bottles (Nalgene). Samples were kept on ice in the dark until further processing (within 2 days). Hydrographic data, including dissolved oxygen (DO), specific conductivity, pH, chlorophyll-a fluorescence (Chl-*a*), and water temperature, were measured using a CTD (Seabird) and two YSI sondes. Water samples were filtered through pre-combusted 0.7 µm GF/F (Whatman) and stored in pre-combusted (550°C) glass vials for DOC

analysis and in acid washed, triple-rinsed, HPDE bottles (Nalgene) for CDOM and EEM measurements. DOC samples were acidified with concentrated HCl to a pH≤2. Both DOC and CDOM samples were stored at 4°C until analysis (within two weeks).

2.3.3 Measurements of DOC and UV-vis absorption

Concentrations of DOC were measured with a Shimadzu TOC-L analyzer equipped with an ASI-L autosampler using the high temperature combustion method (Guo and Santschi 1997). Prior to analysis, samples were extensively sparged with zero air for >5 minutes to remove inorganic carbon. Three to five replicate measurements of 150 μL each were made for each sample. Blanks, including water blanks and instrument blanks, were usually <2 μM-C and compensated from the original measurements accordingly. Detection limit was ≤1 μM and precision was ≤2% in terms of coefficient of variance. Calibration curves were generated before analysis and ultra-pure water, internal standards, and certified DOC standards (University of Miami) were measured every eight samples for quality assurance (Zhou and Guo 2012).

UV-visible absorption spectra were measured with a spectrophotometer (Agilent 8453) using a 1 cm path-length quartz cuvette over a wavelength range of 190-1,100 nm with 1 nm increments. Samples were diluted with ultrapure water to an absorbance value of $\leq$ 0.02 at 260 nm to minimize inner-filtering effects (Zhou and Guo 2012). Ultrapure water was scanned as a blank before samples analysis daily. The water blank was subtracted and the refractive index effect was corrected by subtracting the averaged absorbance between 650 and 800 nm (Stedmon et al. 2000; Zhou and Guo 2012). Absorption coefficients at wavelength λ ($a_{(\lambda)}$, in m^{-1}) were calculated as $a_{(\lambda)} = 2.303A(\lambda)/L$, where $A(\lambda)$ is the absorbance at wavelength λ (nm), and L is the cuvette path-length (in m). Specific UV absorbance at 254 nm ($SUVA_{254}$) was calculated as A_{254}/DOC concentration, resulting in a dimension of m^{-1}/mg-C/L or L/mg-C/m. Spectral slope

through linear fit of the logarithm of absorption coefficients over the wavelength interval of 275-295 nm ($S_{275-295}$) was calculated to provide information on DOM molecular weight and the influence of terrigenous DOM inputs (Helms et al. 2008). Spectral slope has been found to negatively correlate with DOM molecular weight, or the higher molecular weight DOM has a lower spectral slope value.

2.3.4 Measurements of fluorescence EEMs and PARAFAC Modeling

Fluorescence excitation emission matrices (EEMs) were measured using a Horiba Fluoromax-4 spectrofluorometer. Samples were diluted with ultra-pure water to an absorbance value of $\leq$0.02 at 260 nm to minimize inner-filtering effects (Zhou and Guo, 2012). Each sample was scanned from excitation wavelength 220-480 nm with 2 nm increments and emission wavelength 240-600 nm with 1 nm increments in a 1 cm path-length quartz cuvette. The bandpass width was 5 nm for both excitation and emission. A water blank was subtracted from each sample and areas affected by Rayleigh and Raman scattering peaks were eliminated by setting data to zero. The fluorescence index (FIX), an indicator of DOM source and freshness, was calculated as the ratio of emission wavelengths 450 and 500 nm, obtained at excitation wavelength 370 nm (McKnight et al. 2001). The biological index (BIX), another indicator of DOM source, was calculated as the ratio of emission intensity at 380 nm divided by the emission intensity maximum observed between 420 and 435 nm, obtained at excitation wavelength 310 nm (Parlanti et al. 2000). The humification index (HIX), which provides insight into the degree of DOM humification, was calculated as the area under the emission spectra 435-480 nm divided by the peak area under the emission spectra 300-345 + 435-480 nm, at excitation wavelength 254 nm (Ohno 2002).

PARAFAC modeling was done with MATLAB software using the DOMFlour Toolbox (Stedmon and Bro 2008). Sample matrices were calibrated, corrected, and normalized to maximum fluorescence intensity (excluding water scattering peaks) before analysis. A non-negativity outlier test was performed and no samples were identified and subsequently removed as outliers. A split-half analysis was performed for model validation.

2.3.5. Statistical and spatial analyses

Statistical analyses (e.g. ANOVA, T-Test, significance) were performed with Sigmaplot software (version 12.5). Contour maps were generating using Surfer 12 (Golden Software) using the kriging method.

2.4 Results and Discussion

2.4.1 Hydrological features of Green Bay

During June 2014, Green Bay had yet to fully thermally stratify and water temperature ranged from 11.1 to 22.1°C with an average of 15.7±2.7°C. In contrast, by August the bay was fully stratified and the average water temperature was 22.0±0.7°C, which was significantly warmer than June (p <0.0001, Appendix A). As a result, DO concentrations were highly variable between the two sampling months. In June, DO was regulated predominantly by temperature in both surface and subsurface water, as indicated by a significant negative correlation (r^2 = 0.7532; p <0.0001, Appendix A). Conversely, a much less significant, positive relationship existed between water temperature and DO in August (r^2 = 0.0829; p = 0.0314, Appendix A). Further, bottom water DO level was as low as 2.6 mg L^{-1} and an apparent hypoxic zone had developed in the colder bottom waters of the bay (Fig. 2), accompanied by an increase in phosphate concentration in deeper waters in central Green Bay (Lin et al., 2016). This is likely related to

increased sediment oxygen demand and reduced mixing of aerated surface water resulting from thermal stratification of the water column as well as the degradation of DOM in the water column (Klump et al. 2009; also see discussion below).

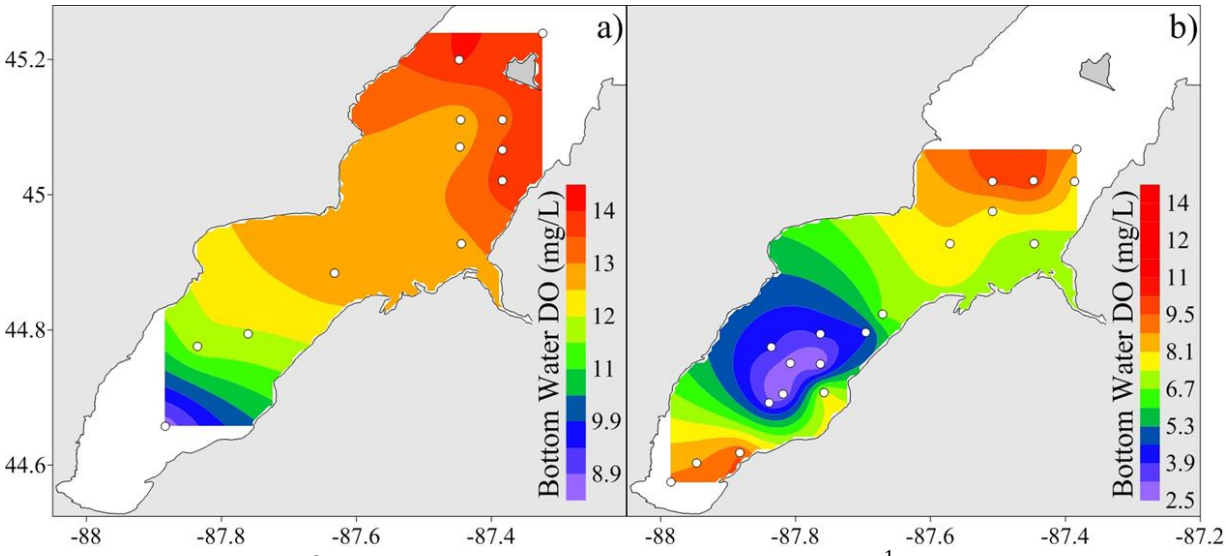

Figure 2: Distribution of bottom water dissolved oxygen (DO, mg L^{-1}) in June (a) an August 2014(b) highlighting the hypoxic zone in Green Bay that developed in August but was not present in June

Surface distributions of specific conductivity (Figs 3a and 3e), which can be used as a tracer of river water inputs due to its conservative mixing behavior, highlight significant differences in hydrology between June and August (Modlin and Beeton, 1970). Surface distributions of specific conductivity in June were consistent with previous observations indicating the presence of the Fox River plume (Lathrop et al. 1990). The Fox River discharges into Green Bay at the southernmost end and is the predominant river input into the bay (Mortimer 1978). The river flow deflects east due to the Coriolis force as it moves north and mixes with open bay water. Additionally, the combination of the Coriolis force and prevailing winds have also been shown to induce a compensating southward flow of open Lake Michigan water along the west coast of the bay, which was evident due to a strong specific conductivity

gradient along both the north-south and east-west axes of the bay (Martin et al. 1995). Conversely, specific conductivity was elevated along the western coast of the bay in August, suggesting temporal variations in Green Bay's hydrological cycle.

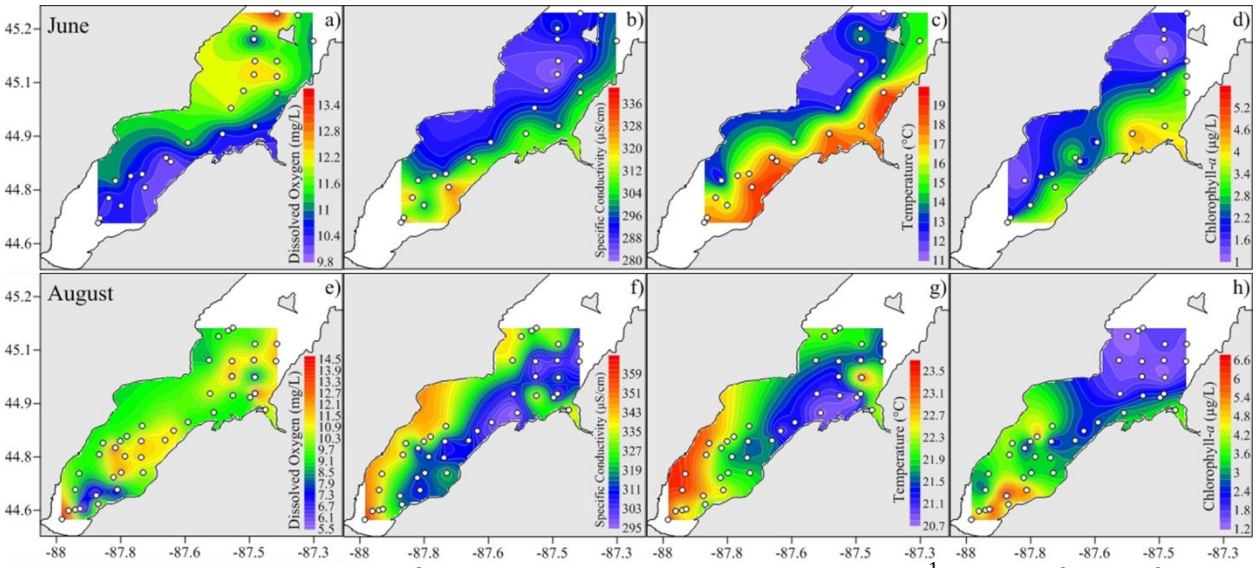

Figure 3: Spatial distributions of (a and e) dissolved oxygen (DO, mg L^{-1}), (b and f) specific conductivity (µS cm^{-1}), (c and g) surface water temperature (°C), (d and h) and chlorophyll-*a* (Chl-*a*, µg L^{-1}) in Green Bay during June (upper panels) and August (lower panels) 2014.

Although Chl-*a* concentrations were not significantly different between the two sampling months (p = 0.261), spatial distributions were somewhat variant (Figs. 3d and 3h). While Chl-*a* was highest at the southernmost sample stations for both months, Chl-*a* was elevated west of Sturgeon Bay in June, but was highly concentrated in the southeastern portion of the bay in August in the same region as the surface water DO minimum (Fig. 3f), suggesting DO consumption from organic matter degradation. However, no such trend was observed in June (Fig. 3b).

2.4.2 DOC abundance and distribution

DOC concentrations ranged from 202 to 561 μM-C with an average of 361±73 μM-C in June, and from 279 to 610 μM-C with an average of 349±64 μM-C in August. No significant difference of DOC abundance between June and August was observed (p = 0.343) (Appendix B). In both months, the highest DOC concentrations were observed in the lower Fox River (546 - 610 μM) and the lowest concentrations were found at the northernmost sampling stations influenced with waters from Lake Michigan (Figs. 4a and 4e). Although DOC concentration was slightly higher in the Fox River in August than June (610 vs. 546 μM), potentially due to dilution by high river discharge in June, DOC concentrations were elevated farther north in the bay in June than August, likely also a result of ~2.5 times higher Fox River discharge in June than August (251 m^3 sec^{-1} vs. 92 m^3 sec^{-1}; Data from USGS gauging station 040851385). This highlights the importance of river inputs on temporal DOC dynamics in Green Bay. Also apparent in Green Bay were low DOC concentrations along the northwestern coast of the bay, concurrent with low specific conductivity suggesting the influence of open Lake Michigan water, which is significantly lower in DOC (average of 154 μM-C in June and July, 2013; Zhou et al., 2016). This supports previous observations and indicates the importance of the surface water hydrology and water mixing with open Lake Michigan water on DOC dynamics in Green Bay (Martin et al. 1995; Mortimer 1978; Modlin and Beeton, 1970).

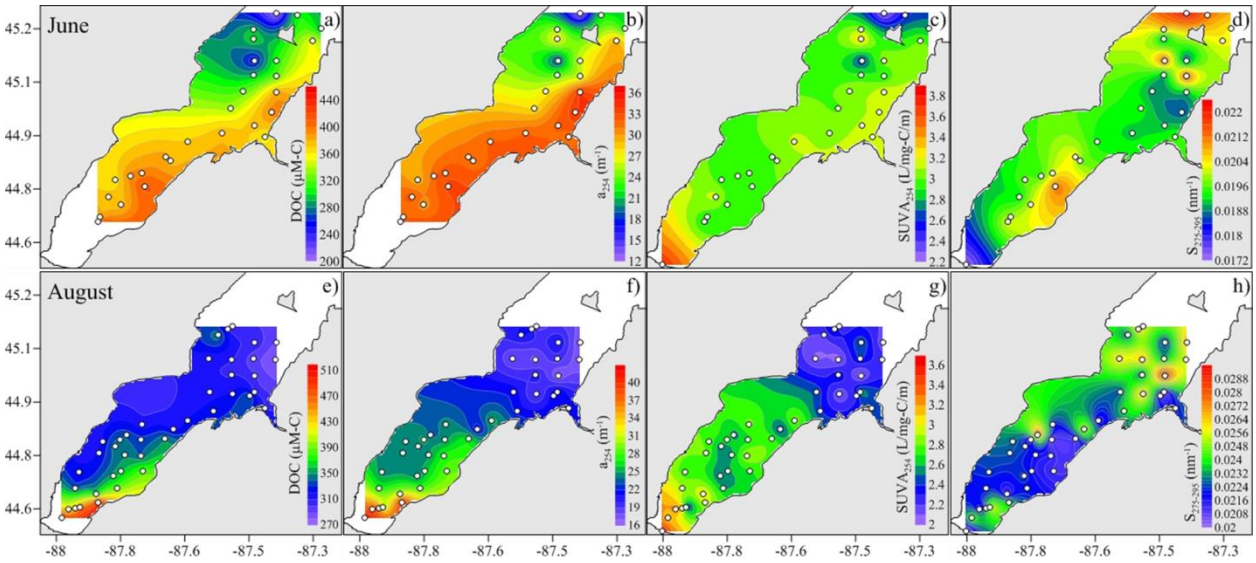

Figure 4: Spatial distributions of dissolved organic carbon (DOC, μM-C), absorption coefficient at 254 nm (a_{254}, m^{-1}), Specific UV absorbance at 254 nm ($SUVA_{254}$, L mg-C^{-1} m^{-1}), and spectral slope between 275 and 295 nm ($S_{275-295}$, nm^{-1}) in Green Bay during June (upper panels) and August (lower panels) 2014.

2.4.3 Variations in CDOM characteristics

The absorption coefficient at 254 nm (a_{254}) ranged from 12.4 to 58.5 m^{-1} (average = 27.9±9.3 m^{-1}) in June and from 16.8 to 59.8 m^{-1} (average = 24.7±8.1 m^{-1}) in August. Values of a_{254} were significantly greater in June than those in August (p = 0.028), showing higher chromophoric DOM components in June. Significant correlation was observed between a_{254} and DOC, both in June (r^2 = 0.9408; p <0.0001) and August (r^2 = 0.8968; p <0.0001), indicting similar chromophoric DOM sources in Green Bay throughout the summer. In addition, spatial distributions of a_{254} resembled those of bulk DOC in both months (Figs. 4b and 4f). The correlation coefficient between a_{254} and DOC was slightly higher in June than August, further attesting to the dominance of riverine inputs to DOC dynamics in June and suggesting alternative DOM sources, for example, from *in situ* production in August (Appendix B).

In both June and August, the Fox River was a source of highly aromatic DOM, as indicated by elevated $SUVA_{254}$ values ranging from 2.2 to 3.8 L mg-C^{-1} m^{-1} (average = 2.9±0.4 L mg-C^{-1}

m^{-1}) in June, and from 2.02 to 3.55 L mg-C^{-1} m^{-1} (average = 2.59±0.34 L mg-C^{-1} m^{-1}) in August. Higher $SUVA_{254}$ values were found in June possibly associated with a higher influx of terrestrial DOM. A distinct south to north gradient was also apparent in both months (Figs. 4c and 4g) suggesting rapid mixing of river and bay waters.

Elevated $S_{275-295}$ values were located in the same region where Chl-*a* was highly concentrated and DO was lowest in concentration suggesting DO consumption from organic matter degradation (Figs 3h and 3e, respectively). Values of $S_{275-295}$ ranged from 0.0173 to 0.0222 nm^{-1} (average = 0.0197±0.0012 nm^{-1}) in June and from 0.0202 to 0.0292 nm^{-1} (average = 0.0233±0.002 nm^{-1}) in August. In both sampling months, however, $S_{275-295}$ showed irregular distributions, possibly as a result of spatial heterogeneity and *in situ* processes such as production and microbial and photochemical degradation that were non-uniformly affecting DOM molecular weight (Miller and Moran 1997). Higher $S_{275-295}$ values in August indicate an overall lower molecular weight DOM pool. This could result from a variety of factors including decreased terrestrial DOM inputs, increased photodegradation, and additional *in situ* DOM processing. In June, lower $S_{275-295}$ values indicate the Fox River was also a source of higher molecular weight (HMW) DOM (Fig. 4d). However, DOM molecular weight in the southern portion of Green Bay in August appears to be affected by processes other than river-bay mixing, as no distinct south-to-north gradient was observed (Fig. 4h). It seems that both autochthonous and degraded DOM gave rise to an overall higher spectral slope value and thus lower molecular weight DOM pool. Given that DOC concentration does not follow this trend, it is likely that biological activity plays an more important role in altering the composition, and therefore DOM molecular weight in southeastern Green Bay in August (Moran et al., 2000; Amon and Benner, 1996).

Although DOC concentrations were not significantly different between June and August, all derived optical properties, including a_{254}, $SUVA_{254}$, and $S_{275-295}$, showed great differences. This indicates that, while the abundance or quantity of DOM did not vary significantly, its quality and composition did change over the summer. In general, the bulk DOC pool was less chromophoric, less aromatic, and lower in molecular weight in August than in June. Non-chromophoric DOC comprised, on average, ~33% of bulk DOC in June while it comprised up to 47% in August. Lower non-chromophoric DOC abundance in the early summer is consistent with higher riverine or terrestrial DOM inputs which in general have a higher aromaticity compared to open lake waters (Appendix B) and higher average $SUVA_{254}$ values in June compared to August (3.01±0.29 L mg-C^{-1} m^{-1} vs. 2.59±0.34 L mg-C^{-1} m^{-1}). This is in agreement with higher a_{254} values in June and may be potentially attributed to increased photochemical degradation and *in situ* DOM sources as indicated by higher Chl-*a* abundance in August than in June (2.96 ± 1.40 µg L^{-1} vs. 2.38±0.89 µg L^{-1}, and Appendix A).

2.4.4. Bulk DOM sources

By using specific conductivity as a mixing index between Fox River and bay waters and Chl-*a* as a proxy for primary production, it was possible to infer the relative importance of each source on DOC dynamics throughout the summer. In June, DOC was more significantly correlated to specific conductivity ($r^2 = 0.6443$, $p < 0.0001$) than Chl-*a* ($r^2 = 0.3030$, $p = 0.0097$). In contrast, DOC in August was more significantly correlated to Chl-*a* ($r^2 = 0.4098$, $p<0.0001$) than specific conductivity ($r^2 = 0.1260$, $p = 0.0246$), indicating a shift from predominant terrestrial DOM sources in June to more *in situ* DOM sources and/or photochemically degraded and microbially modified DOM in August.

There were, however, two distinct relationships between specific conductivity and bulk DOC in August (Fig. 5a). A highly linear trend ($r^2 = 0.6443$, $p < 0.0001$) existed and spatially corresponded to what has previously been identified as the Fox River plume along the eastern coast of the bay (Fig. 5b). A separate cluster with no significant linear relationship ($r^2 = 0.1313$, $p = 0.2237$) also existed and was spatially located along the western coast of the bay as well as near Sturgeon Bay. Given that specific conductivity is elevated along the western coast of the bay, one possible explanation is that river discharge along the western shore more strongly influenced DOM dynamics in August. For example, In June the Oconto, Peshtigo, and Menominee rivers along Green Bay's west shore collectively comprised ~58% of Fox River discharge. However, in August the same rivers comprised upwards of 80% of Fox River discharge (Data from USGS gauging stations). Therefore, not only was primary production more influential in August, discharge from rivers other than the Fox River also played a significant role in regulating DOM dynamics in August.

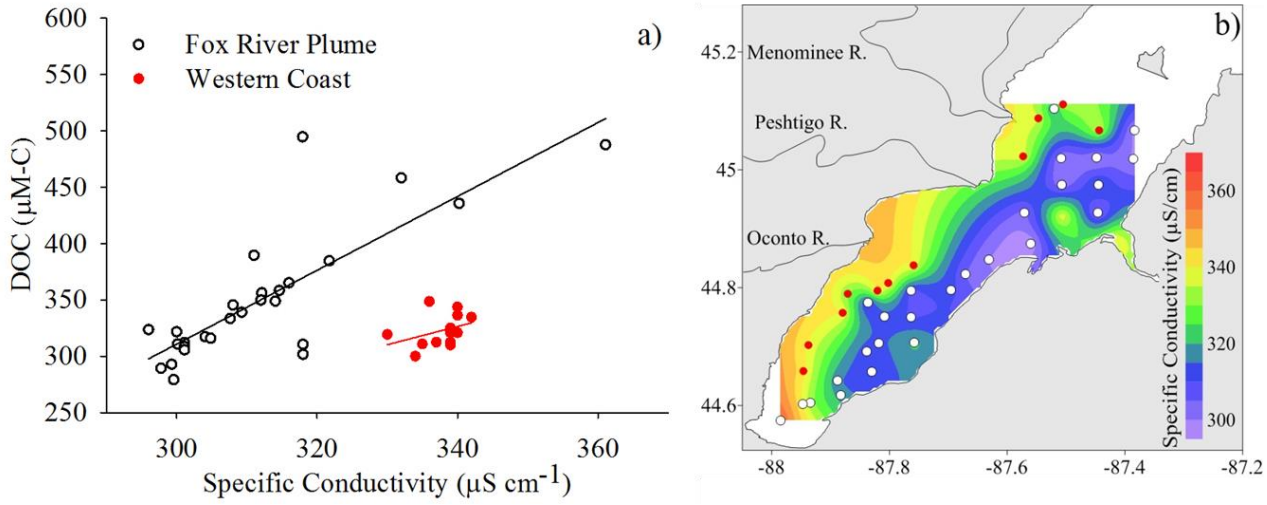

Figure 5. Linear regression between dissolved organic carbon (DOC) and specific conductivity in August (a). Black x's represent sample locations in the Fox River plume while red circles represent sample locations along the western coast and near Sturgeon Bay and are spatially depicted in (b). Fox River Plume – $y=2.0956x-281.1078$, $r^2=0.6443$, $p<0.0001$. Western Coast – $y=1.6178x-223.6927$, $r^2=0.1313$, $p=0.2237$

2.4.5. Variations in excitation-emission matrix characteristics and fluorescence indices

Fluorescence EEMs in Green Bay waters resembled typical spectra for natural DOM samples with distinct terrestrial humic-like peaks A and C and protein-like peaks T and B (Coble 2007) (Fig. 6). In June, peak A was significantly more abundant than August ($p = 0.049$) while peak T was significantly less abundant ($p = 0.0161$), indicating the increased importance of *in situ* produced DOM in August, which is in agreement with increased Chl-*a* concentrations in August (Fig. 6). However, peaks C and B were not significantly different month to month suggesting the moieties producing these peaks did not vary temporally. Further, in June both terrestrial and *in situ* DOM peaks were most abundant in the Fox River. In August only terrestrial humic-like peaks were most abundant in the Fox River, suggesting a temporal change in riverine DOM composition. Protein-like peaks were most abundant at station GB6E, located in the southeastern portion of the bay in close proximity to the Chl-*a* maximum.

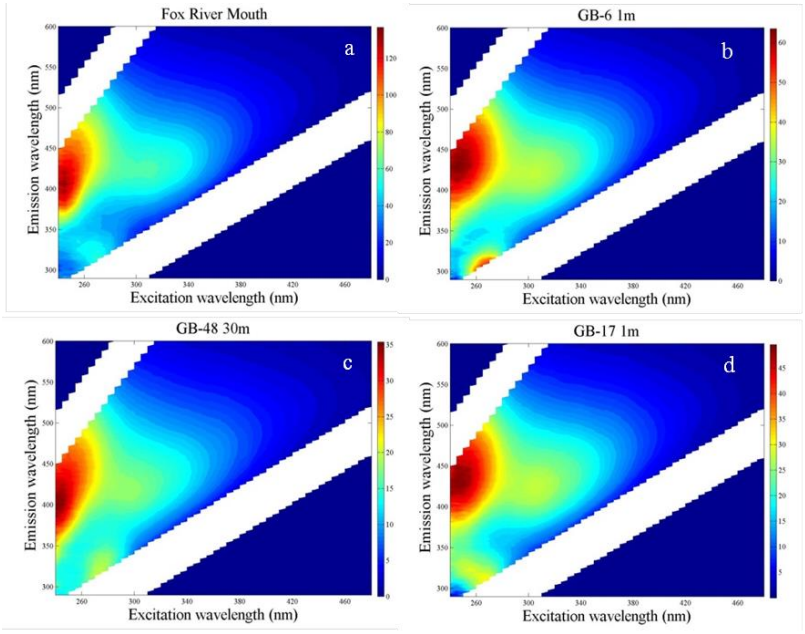

Figure 6: Examples of excitation-emission matrices (EEMs) from a) the Fox River mouth, b) the chlorophyll-a (Chl-*a*) maxima, c) bottom water (30 m) at Station GB-48, and d) surface water (1 m) at Station GB-17.

The HIX value, an indicator of the degree of DOM humification (Ohno 2002), was significantly higher in June (average 2.33±0.65) than August (average 1.68±0.59) (p <0.0001; Appendix C) suggesting that terrestrial DOM was more abundant in June which is in agreement with higher a_{254} and discharge from the Fox River discussed above. The BIX, which indicates the contribution of autochthonous or freshly produced DOM, was significantly higher in August (average 0.73±0.02) than June (average 0.68±0.03) (p <0.0001) indicating increased importance of *in situ* produced DOM in August. The FIX is also an indicator of DOM source, with higher values (~1.8) indicating DOM from the extracellular release and leachate from bacteria and algae and lower values (~1.2) related to terrestrial DOM sources (McKnight et al. 2001). In both months, the average FIX value was low, 1.14±0.03 in June and 1.17±0.02 in August (Appendix C), respectively indicating a dominant terrestrial source in Green Bay regardless of month. Yet, the FIX was still significantly higher in August than June (p <0.0001) suggesting that although terrestrial DOM was predominant, autochthonous DOM was more influential to the bulk DOM pool in August.

In comparison, the contribution of freshly produced DOM in Green Bay was lower than those reported for the Yangtze River Estuary, another anthropogenically stressed system, but DOM humification was greater (Sun et al., 2014 and Table 1). In relation to the rest of the Laurentian Great Lakes, DOM humification in Green Bay was consistently higher than open Lakes Superior, Lake Michigan, and Lake Huron (Zhou et al., 2016 and Table 1). However, it was less than those in the lower Great Lakes, including Lake Erie and Lake Ontario in August (Table 1). On the other hand, freshly produced DOM in Green Bay, indicated by BIX values, was consistently lower than the Great Lakes as a whole (Table 1). Average FIX values were also

lower in Green Bay than all other Great Lakes (Zhou et al. 2016 and Table 1). Overall, DOM in Green Bay seemed to contain more degraded components than open lake waters where *in situ* production could be more dominant.

Table 1: Comparison of the values of the humification index (HIX), the biological index (BIX), and the fluorescence index (FIX) between Green Bay, the Laurentian Great Lakes, and the Yangtze River estuary. Values are averages ± 1 standard deviation.

Site	HIX	BIX	FIX	Reference
Green Bay (June)	2.33 ± 0.65	0.68 ± 0.03	1.14 ± 0.03	This study
Green Bay (August)	1.68 ± 0.59	0.73 ± 0.02	1.17 ± 0.02	"
Lake Superior	1.13 ± 0.02	0.91 ± 0.06	1.14 ± 0.02	Zhou et al. (2016)
Lake Michigan	1.28 ± 0.25	0.89 ± 0.03	1.19 ± 0.01	"
Lake Huron	1.23 ± 0.28	0.90 ± 0.06	1.21 ± 0.02	"
Lake Erie	1.98 ± 0.59	0.91 ± 0.02	1.22 ± 0.02	"
Lake Ontario	1.91 ± 0.68	0.92 ± 0.03	1.22 ± 0.02	"
Yangtze River Estuary	1.10 ± 0.39	1.16 ± 0.23	No data	Sun et al. (2014)

2.4.6. Variations in fluorescent DOM components derived by PARAFAC analysis

Four PARAFAC-derived fluorescent-DOM components were identified each sampling month, with slight differences in Ex/Em wavelength (Table 2 and Fig. 7). Two of the components have been previously identified as terrestrial humic-like (C1 and C3 in June, and C1 and C4 in August) (Stedmon and Markager 2005; Yamashita et al. 2008; Cory and McKnight 2005). One component has previously been identified as aquagenic humic-like (C2 in both months) (Guéguen et al. 2011; Coble 2007), and one peak has been identified as protein-like (C4 in June and C3 in August) (Yamashita et al. 2008; Cory and McKnight 2005). Detailed descriptions of the PARAFAC-derived fluorescent-DOM components are given in Table 2.

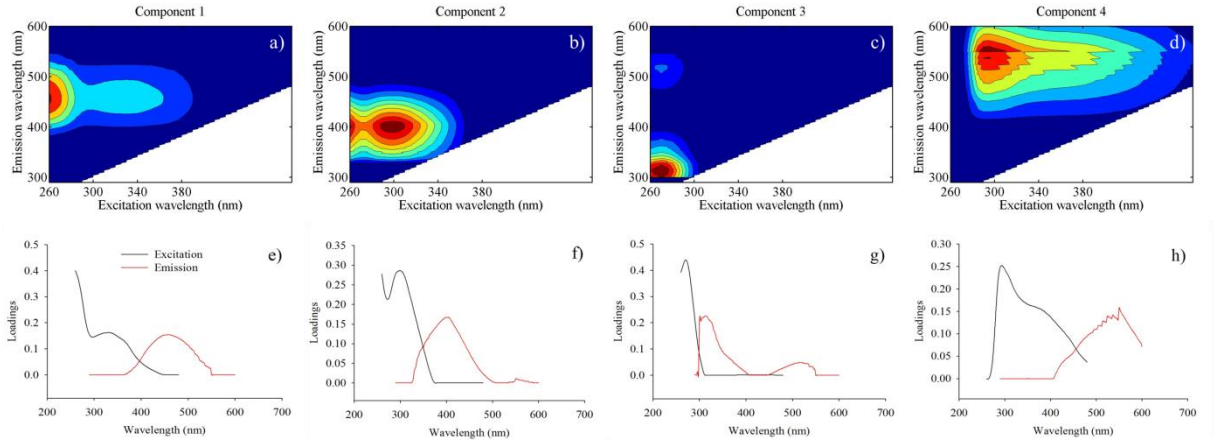

Figure 7: Excitation-emission plots of fluorescent-DOM components identified by PARAFAC analysis in both June and August (See Table 2 for specific Ex/Em data of each component). In June, components 1 and 3 were terrestrial humic-like, component 2 was aquagenic humic-like, and component 4 was protein-like. In August, components 1 and 4 were terrestrial humic-like, component 2 was aquagenic humic-like, and component 3 was protein-like.

Table 2: Description of PARAFAC-derived fluorescent-DOM components in Green Bay during June and August 2014.

June Ex/Em (nm)	August Ex/Em (nm)	Component Description
C1 – 255 (310)/440	C1 – 250 (315)/458	Similar to Peak A - UVC humic like. Dominates export from natural catchments and exported from agricultural catchments. Allochthonous.
C2 – 240 (290)/354	C2 – 240 (300)/392	Similar to Peak M – marine humic-like. May be allochthonous, autochthonous, or a result of microbial activity.
C3 – 285/508	C4 – 280/508	UVA humic like. High molecular weight and aromatic. Fluorescence resembles fulvic acid. Widespread.
C4 – 265/312	C3 – 270/316	Similar to Peak B – Tyrosine-like. May indicate amino acids, free or bound proteins, and may indicate more degraded peptide material.

Humic like DOM was more abundant early in the summer while protein –like DOM became more dominant in August indicating a shift from a predominant terrestrial source in June to a more biologically controlled system in August. In June, both terrestrial humic-like DOM components were highly correlated with each other (r^2 = 964, p <0.0001) (Figs. 8a and 8c) and with bulk DOC (r^2 = 0.772, p <0.0001 and r^2 = 0.764, p <0.0001) suggesting their source was

from Fox River discharge. Elevated abundance of aquagenic humic-like DOM north of Sturgeon Bay along the eastern shore suggests the presence of an alternative source other than the Fox River (Fig. 8b). Conversely, the aquagenic humic-like component was not elevated north of sturgeon bay in August suggesting temporal variations in its source and cycling mechanisms (Figs. 8e, 8f, and 8h). Differences in the spatial distribution of protein-like DOM were evident between June and August (Figs. 8d and 8g) and may be linked to nutrient availability regulated by Fox River discharge. When Fox River discharge was high early in the summer and the plume migrated farther north, protein-like DOM was abundant farther north. Later in the summer when discharge decreased, protein-like DOM was most abundant in the southern bay in close proximity to the Chl-*a* maxima attesting its biological origin. Warmer water temperatures likely promoted increased *in situ* production of protein DOM as well.

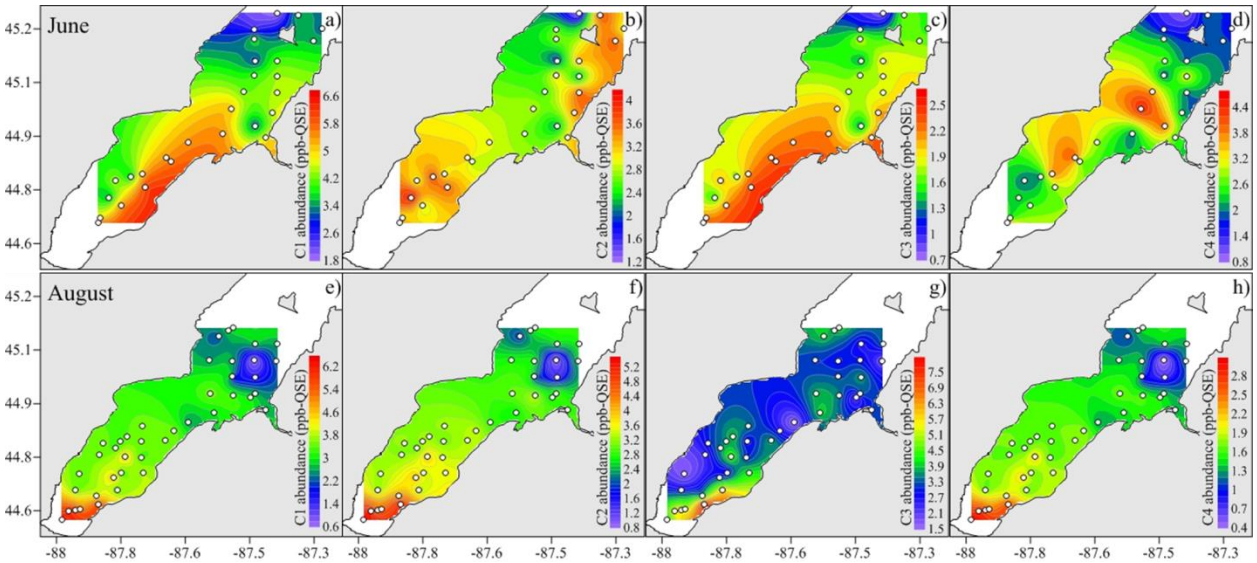

Figure 8: Spatial distributions of PARAFAC-derived fluorescent-DOM components (in ppb-QSE) in June (a-d) and August 2014 (e-h). A more detailed description of each component can be found from Table 2.

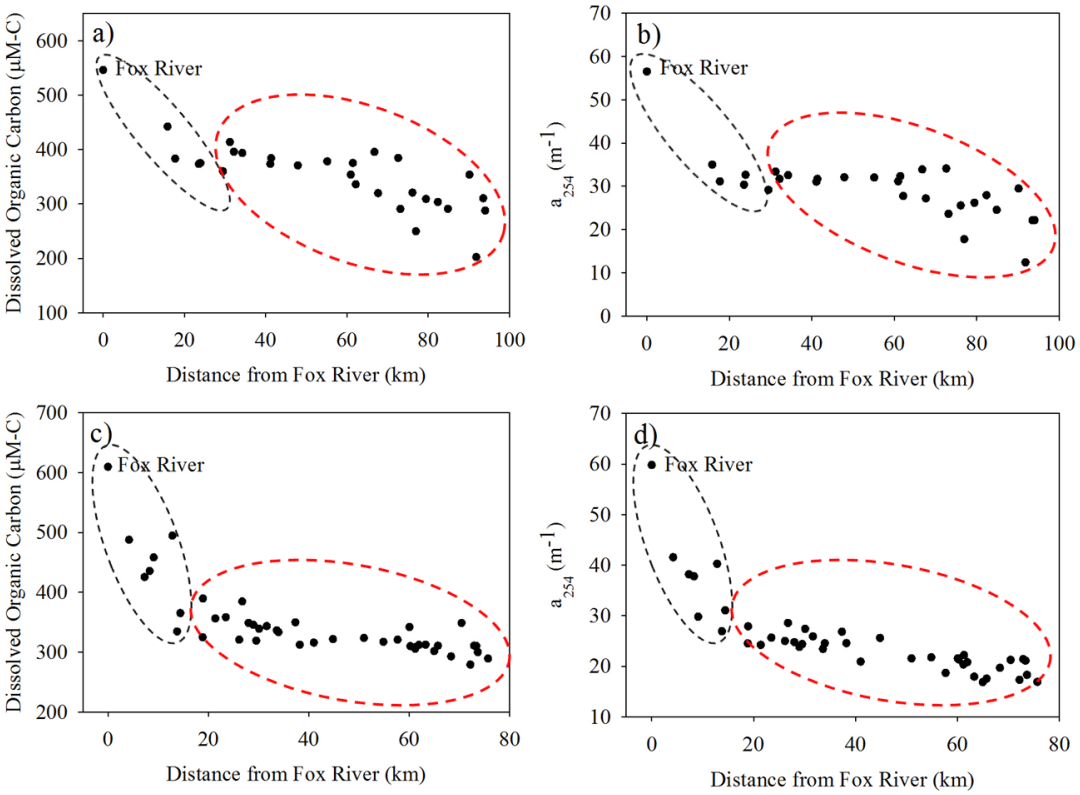

Figure 9: Relationship between distance from the Fox River mouth and DOC concentration in June (a), distance from the Fox River mouth and a_{254} in June (b), distance from the Fox River mouth and DOC concentration in August (c), and distance from the Fox River mouth and a_{254} in August (d) in Green Bay showing two distinct mixing zones. Black circles represent Zone 1 and red circles represent Zone 2.

2.4.7. Behavior of DOM during river-bay water mixing

Previous studies have reported rapid mixing of Fox River water with open Green Bay water in the southern portion of the bay (Klump et al. 2009). As a result, high sedimentation rates occur in the southern bay, removing riverine constituents from the water column at an elevated rate (Klump et al. 1997). Similar patterns were observed in Green Bay in June and August, where two distinct mixing zones were evident (Fig. 9). In June, DOC decreased 27% from ~545 to ~400 µM-C within zone I, which extended 29 km from the Fox River mouth (Fig. 9a). In August, however, DOC decreased 47% from ~610 to ~325 µM-C within zone I which only extended 19 km from the Fox River mouth, likely as a result of lower discharge indicating

temporal variations in mixing behavior (Fig. 9c). In both months, DOC concentration remained fairly constant in zone II. However, greater fluctuation was seen in zone II in June indicating a highly dynamic system while DOC appeared more conservative in zone II in August.

Chromophoric DOM (a_{254}) displayed similar trends with DOC in both months with two distinct mixing zones, but decreases in zone I were much greater. In June, a_{254} decreased 47% from ~57 m^{-1} to ~30 m^{-1} in zone I (Fig. 9b). In August, a_{254} decreased almost 75% from ~60 m^{-1} to ~19 m^{-1} in Zone I suggesting a highly dynamic and reactive nature of CDOM during early mixing of riverine and bay waters (Fig. 9d). Similar to DOC, a_{254} values remained fairly constant in zone II in both months with higher variations in CDOM abundance in June.

Mixing plots based on the relationship between DOC or a_{254} and specific conductivity were used to estimate the apparent removal/addition of DOM and CDOM in Green Bay (Loder and Reichard 1981). The hydrological cycle of Green Bay is complex and is influenced by multiple riverine sources, mixing with Lake Michigan waters, and variable wind patterns (Mortimer 1978; Martin et al. 1995; Waples and Klump 2002). As a result, simple 2 end member mixing of constituents may be difficult to model. With an average addition of less than 10%, bulk DOM and a_{254} mixing plots suggest a conservative mixing behavior of DOM although there were evident DOM additions at most stations in June, likely due to light shielding by high CDOM and thus lower photodegradation and *in situ* production (Figs. 10a and 10b). In August, DOM as a whole appeared less conservative than in June with a removal of ~13%. However, when sample stations were divided into the Fox River plume and the western coast as determined by specific conductivity in Fig. 5, a quasi-conservative mixing behavior of bulk DOC and CDOM was observed with both addition and apparent removal at some individual stations (Figs. 10c and 10d). In August, CDOM removal appears to be much higher than DOC in both the Fox River

plume and along the western coast indicating again a higher reactivity of optically active DOM components, which is further buttressed by higher non-chromophoric DOC relative to June. However, when an averaged endpoint which was more representative of other open Green Bay stations was used to generate the theoretical mixing line, CDOM appeared highly conservative (Fig. 10). Although DOC appeared to behave in a quasi-conservative manner, the composition of DOM underwent significant changes during mixing.

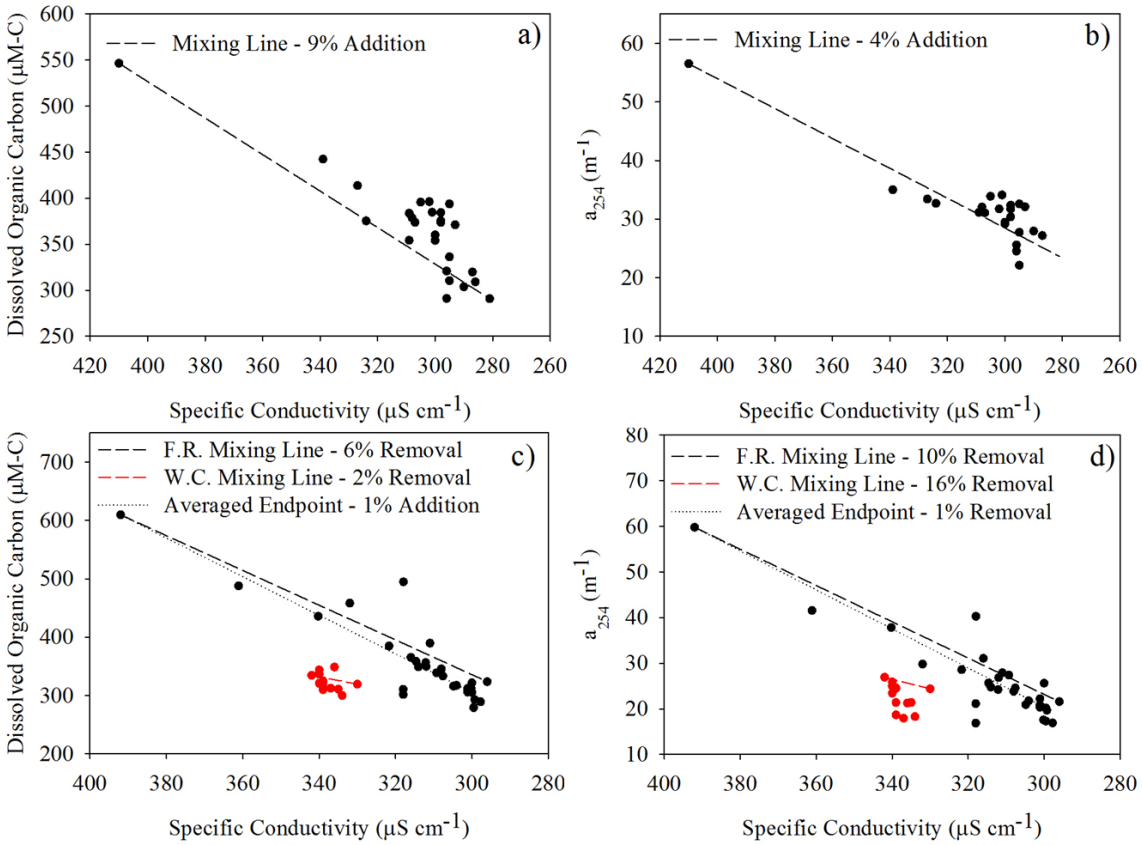

Figure 10: Relationship between dissolved organic carbon (DOC) concentration (µM-C) and specific conductivity (µS cm^{-1}) in Green Bay in June (a), absorption coefficient at 254 nm (a_{254}, m^{-1}) and specific conductivity in June (b) DOC and specific conductivity in August (c), and a_{254} and specific conductivity in August (d). F.R. = Fox River, W.C. = west coast. Mixing lines were derived from the equation of line between the points of lowest and highest specific conductivity. In August, the station with the lowest specific conductivity had higher than usual concentrations of DOC, so an averaged endpoint was also plotted for comparison.

In June, $SUVA_{254}$ values decreased sharply while $S_{275-295}$ increased sharply with distance from the Fox River mouth indicating a rapid decrease in both aromaticity and mean molecular weight of the bulk DOM pool (Figs. 4c and 4d). While $SUVA_{254}$ showed a similar trend in August, no such trend was observed for $S_{275-295}$ indicating other controlling factors besides mixing/dilution were affecting DOM molecular weight such as biological and photochemical degradation of DOM (Figs. 4g and 4h). Regardless, DOM composition appears to be altered the most significantly during early mixing in the southern portion of the bay.

The mixing behavior of individual DOM components relative to specific conductivity also suggests a highly dynamic nature of the DOM pool. In June, the terrestrial humic-like DOM components behaved conservatively with an average removal of only 7%, the aquagenic humic-like component displayed an average removal of 17%, while the protein-like component displayed an addition of 15%. Bulk FDOM, however, behaved conservatively with a calculated removal of <4% between all four components. This, in conjunction with the mixing behavior of DOC, suggests that although bulk DOC appeared to behave conservatively, DOM composition was significantly altered with different extents highlighting the dynamic nature of DOM mixing and cycling in Green Bay in June. In August, all four DOM components underwent significant removal with an average removal of 21%, consistent with higher CDOM removal and higher abundance of non-chromophoric DOC. Contrary to June, the protein-like component C3 displayed a removal of 14% suggesting the rate of microbial degradation was greater than the rate of *in situ* production of DOM.

The conservative nature of terrestrial humic-like components in June may be explained by their refractory nature. The percent contribution of both C1 and C3 increased in the southern bay with distance from the Fox River (Figs. 11a and 11c). Because the Fox River appears to be their

source, this observation can potentially be explained by the removal of other DOM components relative to C1 and C3. Further, C1 and C3 normalized to DOC concentration (C1/DOC and C3/DOC, respectively) both remained relatively constant until as far north as Sturgeon Bay (Figs. 12a and 12c). This suggests that although DOC concentration decreased rapidly with distance from the Fox River, the relative abundance of C1 and C3 did not, further buttressing their similar source and refractory nature (Ishii and Boyer, 2012; Diffey, 2002). No such trend was observed for the other DOM components (Figs. 11 and 12).

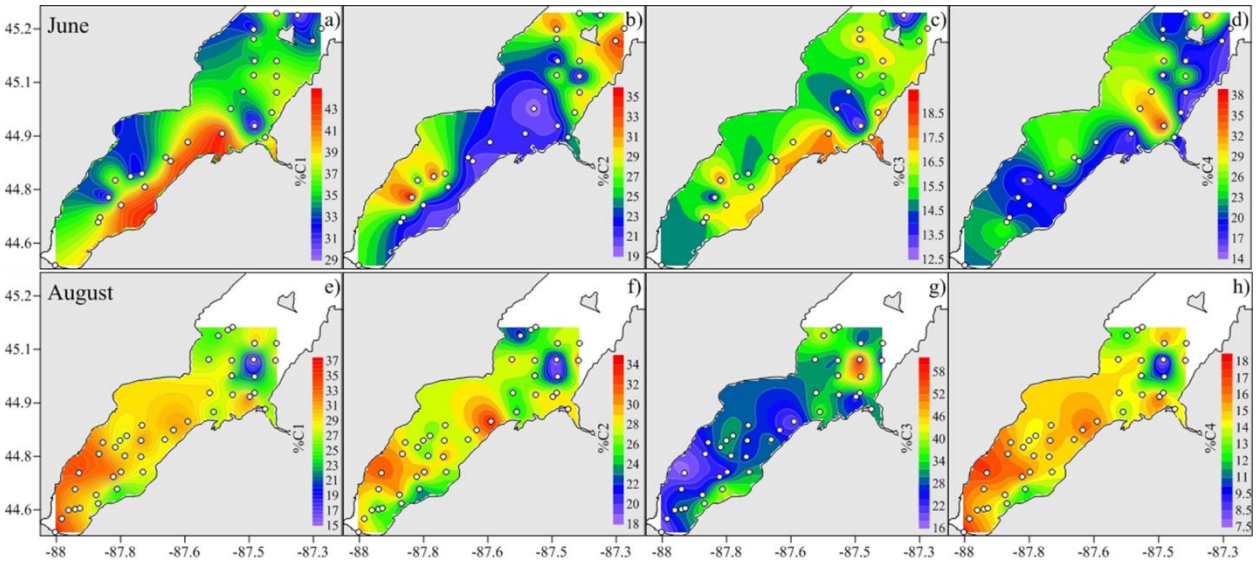

Figure 11: Spatial distributions of the percent contribution of each fluorescent-DOM component to bulk fluorescent-DOM (FDOM) in Green Bay during June (a-d) and August (e-h).

2.5. Conclusions

Dissolved organic carbon dynamics in Green Bay displayed both spatial and temporal variability. Although bulk DOC concentration was not significantly different between June and August, optical characteristics (i.e. a_{254}, $SUVA_{254}$, and $S_{275\text{-}295}$) were, indicating the chemical composition or quality of DOM was different. A significant difference in the percent of non-chromophoric DOC (33% in June and 47% in August) further supports this observation and

indicates a less aromatic and lower molecular weight DOM pool in August. Four similar fluorescent DOM components were identified with PARAFAC analysis in June and August: two terrestrial humic-like, one aquagenic humic-like, and one protein-like DOM. While Green was dominated by allochthonous DOM, *in situ* production was more influential in late summer with more protein-like DOM presence, resulting in changes in chemical composition of the bulk DOM pool. Further, *in situ* production may have influenced dissolved oxygen dynamics and hypoxia development in the southern portion of the bay as a result of heterotrophic oxidation of DOM in the water column. The humification index was significantly higher in June while the biological and fluorescence indices were significantly higher in August. This indicates that the bulk DOM pool was more humified in June and comprised of fresher DOM in August, concurrent with higher concentration of Chl-*a* in August.

Hydrology was also a significant factor influencing both the spatial and temporal variation of DOM. The dominant circulation in the bay (Hamidi et al. 2015) significantly influenced the spatial distribution of DOM, deflecting DOC rich Fox River water along the eastern coast with DOC poor open Lake Michigan waters being transported south along the western coast of the bay. While bulk DOM was generally conservative during estuarine mixing, August displayed unique mixing behaviors between the southern portion of the bay and the western coast, influenced by a significant increase in the discharge of small rivers along the western coast relative to the Fox River. Specifically, each fluorescent DOM component displayed two separate, linear relationships with specific conductivity indicating the increased complexity of DOM sources and sinks in August relative to June. DOM dynamics in Green Bay have unique temporal variation controlled by both allochthonous organic matter loading as well as *in situ* production,

and could be linked to riverine discharge, biological activity, hydrological condition, and dissolved oxygen dynamics in the bay.

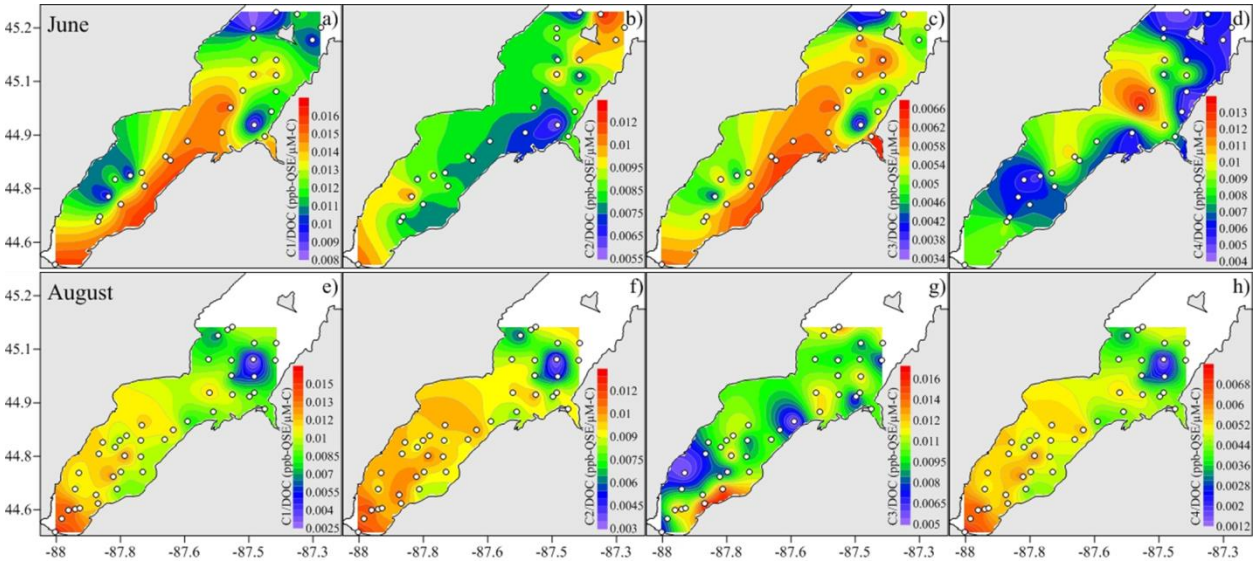

Figure 12: Spatial distributions of PARAFAC-derived fluorescent-DOM components normalized to DOC concentration (C^n/DOC, ppb-QSE/μM-C) in Green Bay during June (a-d) and August (e-h).

3. Part II: Characterization and yields of dissolved organic matter and nutrients excreted by invasive quagga mussels in Lake Michigan

3.1 Background

Since their colonization in Lake Michigan, the invasive quagga mussel (*Dreissena rostriformis bugensis*) has caused unprecedented ecological and environmental changes including a decline in fish biomass, increasing water clarity, food web alterations, and significant changes to carbon and nutrient cycling pathways (Bunnell et al. 2006; Bootsma 2009; Cuhel and Aguilar 2013; Binding et al. 2015; Lin et al. 2016). Quagga mussels have coupled the benthic and pelagic systems through filtering pelagic particulate matter, including phytoplankton and zooplankton, and excreting/egesting nutrients in the benthos (Schindler et al. 2002). Specifically, quagga mussels have been shown to excrete both particulate and soluble inorganic and organic

phosphorus species, ammonia, as well as significantly increase benthic oxygen consumption (Conroy et al. 2005; Bootsma et al. 2012; Ramcharan and Turner 2010; Mosley and Bootsma 2015). Excretion of phosphorus in the nearshore zone has even been linked to nuisance algal blooms which have forced costly beach closures and facilitated the spread of disease (Hecky et al. 2004; Whitman et al. 2003).

It is also evident that quagga mussels have had significant interactions with the organic carbon (OC) pools, most obvious being the exhaustive consumption of particulate organic matter (POM) resulting in increasing water clarity or Secchi depth (Kerfoot et al. 2010; Vanderploeg et al. 2010; Binding et al. 2015). Studies have suggested that quagga mussels have the capacity to consume over half of the annual net primary production in southern Lake Michigan which has, in part, led to a decline in forage fish of 93% since the 1980s (Tyner et al. 2015, Egan 2008). Although changes in food web structure and ecosystem function in Lake Michigan by quagga mussels and their potential interactions with the OC pool are widely recognized, the quantitative role of quagga mussels in the uptake or excretion of dissolved and colloidal organic matter species are largely unknown. Specific cycling pathways of organic matter and nutrient species, quantitative linkages between benthic and water column properties, and the ultimate fate of consumed organic matter by mussels remain elusive.

Dissolved organic matter (DOM) is the largest fraction of active OC in aquatic systems and provide a link between the biosphere, hydrosphere, and geosphere (Biddanda and Cotner 2002; Cole et al. 2007; Bauer and Bianchi 2011). Within the bulk DOM pool, the light absorbing fraction known as chromophoric DOM (CDOM) could have higher photoreactivity and has been widely used as a proxy for the bulk DOM pool (Miller and Zepp 1995; Coble 2007). The source, chemical composition and size of DOM could significantly impact ecological function and

biogeochemical cycling. For example, the molecular size of DOM has been shown to be an important factor in regulating the transport, speciation, bioavailability, and environmental fate of contaminants and trace elements (Wang et al. 1997; Guo et al. 2002; Benner and Amon 2015). Further, the composition of DOM can affect the heterotrophic community, influencing heterotrophic metabolism (Lennon and Pfaff 2005). Despite their importance, knowledge of the dynamics of different carbon species in the Great Lakes remains scarce and changes in carbon dynamics after the colonization of the invasive quagga mussel are largely unknown. Therefore, understanding the interactions between benthic quagga mussels and the DOM pool is vital for understanding changes in biogeochemical cycling pathways of carbon and nutrient species in a changing ecosystem, as well as understanding the impact of invasive species on the Laurentian Great Lakes.

3.2 Purpose of Study

Major objectives of this study were to 1) examine filtration rates and retention efficiency of macromolecular organic matter by quagga mussels using model compounds/nanoparticles; 2) determine the excretion/egestion rates of DOM by quagga mussels through incubation experiments; 3) characterize the size spectrum and organic composition of excreted-DOM from quagga mussels; and 4) identify transformations and cycling pathways of organic matter by quagga mussels in Lake Michigan and provide insight into a better understanding of the role of invasive quagga mussels in regulating the carbon dynamics in the Great Lakes.

3.3 Methods

3.3.1 Mussel and water collection

Quagga mussels were collected onboard the RV Neeskay with a ponar from stations with a water depth of ~50 m in southwestern Lake Michigan, off the coast of Milwaukee. Mussels were thoroughly rinsed with lake water, wrapped in dampened paper towels, placed in plastic bags, and kept in a cooler with ice, but not in direct contact with ice (Baldwin et al. 2002; Conroy et al. 2005). Once in the lab, mussels were kept at ~4°C until incubation experiments (within 24 h).

Large volumes of surface lake water were collected from an open lake station (43º04.5000'N and 87º46.0230'W) for laboratory incubation experiments. Surface water was directly pumped peristaltically through a 0.4 µm polycarbonate cartridge into acid cleaned carboys. The 0.4 µm filtrate was further ultrafiltered through a 1 kDa ultrafiltration cartridge to remove any colloids and particles larger than 1 kDa or 1.2 nm (Guo and Santschi 2007). The <1 kDa filtrate was the used for mussel excretion experiments.

3.3.2 Incubation experiments to determine clearance rate

Prior to incubation, mussels were acclimated to room temperature (22°C) for ~ 24 hours. Mussels were then thoroughly scrubbed with a toothbrush to remove microbes and rinsed in <1 kDa ultrafiltered lake water used for the incubation. Individual mussels were then placed in beakers filled with 200 ml of ultrafiltered lake water spiked with 2 ppm fluorescently tagged, carboxylate modified polystyrene microspheres (Life Technologies), including 20, 100, 200, and 500 nm, and 1 and 2 µm (Table 3) and were covered with aluminum foil to prevent contamination from air born particulates.

Incubations were done with one microsphere size at a time. However, a separate incubation experiment combining both 20 and 500 nm microspheres (representing the lower and upper limits of the operationally defined dissolved phase) with different characteristic excitation-emission (Ex/Em) wavelengths was also conducted to examine whether mussels will selectively

remove a specific sized particle when multiple sizes were available (Fig. 13). This was designed to insure differences in clearance rates were in fact a result of particle size, and not due to other factors (e.g. variations in filtering behavior between different mussels). Incubations of each microsphere size were done in triplicate with a control with no mussel to assess any potential effects of coagulation and precipitation as well as potential adsorptive loss to the beaker wall.

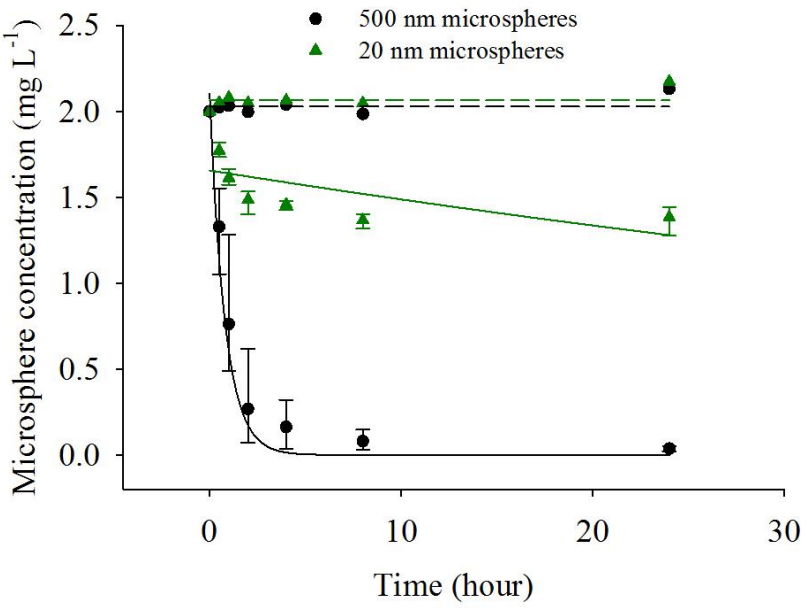

Figure 13: Clearance kinetics for the 0.02 and 0.5 µm particles. Both size particles were combined in the same experimental beaker and dotted lines represent the control with microspheres but no mussels. Details of the microspheres used are listed in Table 3.

Incubations were carried out in a dark room to mimic benthic conditions as well as to prevent photobleaching of the fluorophore tags on microspheres. Time series samples were collected at 0, 0.5, 1, 2, 4, 8, and 24 h and began once mussels started filtering. Before sample collection, air was gently bubbled into the beaker to homogenize the solution and ensure the beakers had sufficient dissolved oxygen. Microsphere concentration in each sample was determined fluorometrically with a Horiba Fluoromax4 spectrofluorometer targeting the specific Ex/Em wavelength of the fluorescent tag (Table 3). Removal rates were calculated by assuming

first-order removal (i.e. $A=A_o e^{(-\lambda t)}$). Removal residence time was taken as $1/\lambda$, where λ represents F/V (F = volume/time in L hr^{-1} and V = volume in L) (Haye et al. 2006).

Table 3: Size and fluorescence excitation/emission wavelengths for microspheres used in clearance rate incubations. All microspheres were carboxylate modified, polystyrene spheres from Life Technologies™.

Microsphere Size (µm)	Color (Ex/Em wavelength (nm))	Cat #
0.02	Nile red (535/575) and red fluorescent (580/605)	F8784 F8887
0.1	Red fluorescent (580/605)	F8887
0.2	Red fluorescent (580/605)	F8887
0.5	Red fluorescent (580/605)	F8887
1	Red fluorescent (580/605)	F8887
2	Red fluorescent (580/605)	F8887

3.3.3 Excretion of DOM and nutrients

All incubation experiments were carried out in 600 ml beakers filled with 500 ml of ultrafiltered lake water and were covered with foil to prevent contamination from air born particulates. Cleaned mussels were sorted into three different size classes: namely 5-15 mm, 15-25 mm, and >25 mm. Two replicates of the 5-15 mm class with 20 mussels per beaker, 6 replicates of the 15-25 mm class with 10 mussels per beaker, and 2 replicates of the >25 mm class with 10 mussels per beaker were sampled for a total of 10 replicates. A control with no mussels was also sampled and no significant differences were found for all measured parameters throughout the incubation. The number of replicates for each size category was determined based on the size distribution and quantity of collected mussels. Samples for the measurements of dissolved organic carbon (DOC) (see section 2.3.3 for methodology), total dissolved nitrogen (TDN), carbohydrates (CHO), UV-visible absorbance (see section 2.3.3 for methodology), and fluorescence (see section 2.3.4 for methodology) were filtered through a 0.7 µm GF/F syringe

filter (Whatmann). Samples for phosphorus (P) analysis were filtered through a 0.45 µm polycarbonate membrane syringe filter (Whatmann). Dissolved organic carbon and TDN samples were collected at 0, 2, 4, 8, 24, and 48 h, transferred into pre-combusted glass vials, immediately acidified with concentrated HCl to a pH of <2, and stored in a refrigerator until analysis. Samples for carbohydrates, UV-vis absorbance, and fluorescence analysis were collected at 0, 0.5, 1, 2, 4, 8, 24, and 48 h, transferred to acid washed centrifuge tubes, and stored in a refrigerator until analysis. Samples for P were collected at 0, 2, 4, 8, 24, and 48 h, transferred to acid washed, 30 ml HPDE bottles (Nalgene), and stored in a freezer until analysis.

After the incubation, the remaining solution from each beaker was combined, homogenized, and filtered through duplicate pre-combusted 0.7 µm GF/Fs (Whatman) for the analysis of particulate OC (POC) , and a 0.45 µm polycarbonate filter (Millipore) for total suspended solids (TSS), respectively. The filtrate was stored in an acid washed, 125 ml HPDE bottle (Nalgene) in a refrigerator for the analysis of DOM size distribution using flow field-flow fractionation.

Excretion rates were converted to mass-specific excretion rates (i.e. µmol $mgDW^{-1}$ d^{-1}) using a length-weight relationship from the same region of Lake Michigan (Mosley and Bootsma 2015): $DW = 0.0035 \times L^{2.78}$ where DW denotes dry weight (mg) and L denotes length (mm), which was applied to the average mussel length for each replicate.

3.3.4. Measurements of nitrogen and carbohydrate species

Total dissolved nitrogen was measured with the 720°C catalytic thermal decomposition/chemiluminescence method with a Shimadzu TNM-L analyzer. Similar quality assurance/control was applied to TDN analysis (section 2.3.3). The detection limit was <1 µM. Precision was set at a coefficient of variance of ≤2%.

Carbohydrate (CHO) species including monosaccharides (MCHO), dilute acid-hydrolysable carbohydrates (HCl-CHO) and total carbohydrates (TCHO) were directly measured using a modified version of the 2,4,6-tripyridyl-s-triazine (TPTZ) spectrophotometric method (Hung et al. 2001; Lin and Guo 2015). The dilute acid-hydrolysable polysaccharides (HCl-PCHO) were determined as the difference between dilute acid-hydrolysable CHO (HCl-CHO) and MCHO (i.e. HCl-PCHO = HCl-CHO – MCHO). Dilute acid-resistant polysaccharides (HR-PCHO) were determined as the difference between TCHO and HCl-PCHO (i.e. HR-PCHO = TCHO – HCl-PCHO).

For MCHO species, 1 ml of sample was mixed with 1 ml $K_3^-(Fe(CN)_6)$ in a Teflon vial and placed in an oven at 115°C for 30 min. Next, 1 ml of $FeCl_3$ in acetic acid buffer and 2 ml of TPTZ solution was added in a dark room, as color formation is light sensitive. After 30 min, the absorbance was measured at 595 nm. Measurements of HCl-PCHO were done by digesting 2 ml of sample in 0.2 ml 1M HCl at 100°C for 24 h. The samples were then neutralized with 0.2 ml 1M NaOH. After digestion and neutralization, samples were measured according to the MCHO protocol. Measurements of TCHO were done by lyophilizing 4 ml of sample followed by digestion with 0.4 ml of 12M H_2SO_4 for 2 h at room temp. Next, 3.6 ml of E-pure H_2O was added to return the sample to its original volume and 2 ml of that sample was pipetted into a Teflon vial and placed in an oven at 100°C for 2 h (Lin and Guo 2015). The sample was then neutralized with 0.64 ml of 8M NaOH and processed according to the MCHO protocol.

3.3.5 Analysis of dissolved organic and inorganic phosphorus species

Total dissolved phosphorus (TDP) samples were digested with persulfate solution at 95° C for 24 h (Huang and Zhang 2009; Lin et al. 2012) and were subsequently measured using the standard phosphomolybdum blue method using a spectrophotometer (Agilent 8453) and a 5 cm

cuvette at a wavelength of 882 nm (Hansen and Koroleff 1999). Dissolved inorganic phosphorus (DIP) was directly measured without persulfate digestion. Dissolved organic phosphorus (DOP) was determined as the difference between TDP and DIP (i.e. DOP = TDP – DIP).

3.3.6 Analysis of DOM size distribution

The continuous size distribution of DOM excreted by quagga mussels was determined with an asymmetrical flow field-flow fractionation (FlFFF) system (AF2000, Postnova) coupled online with two fluorescence detectors (Shimadzu RF20A, with Ex/Em at 275/340 nm and 350/450 nm to track protein-like and humic-like DOM components, respectively) and a UV-vis detector (Postnova SPD20A, set at 254 nm). The theory of FlFFF is described in detail elsewhere (Giddings 1993) and specific calibration and procedures are described in Zhou and Guo (2015). Briefly, FlFFF is a chromatography-like technique that produces a continuous size distribution of colloids based on their diffusion against a liquid crossflow in an open channel (Baalousha et al. 2011). The lower wall of the channel was covered with a 300 Da ultrafiltration membrane allowing any material <300 Da to be removed from the channel. The relationship between FFF retention time and diffusion coefficient (*D*) was determined graphically using protein standards with known *D* (Stolpe et al. 2010; Zhou and Guo 2015). The hydrodynamic diameter was calculated from *D* based on the Stokes relation. Specific details can be found in Stolpe et al. (2010). Diffusion coefficient was also converted to molar mass (MW) by calibration with polystyrene sulfonate (PSS) standards (Beckett et al. 1987).

3.4 Results and discussion

3.4.1 Clearance rates of macromolecules and microparticles by quagga mussels

Clearance rates derived from the 20, 100, and 200 nm spherical particles, which are in the operationally defined dissolved phase, were significantly lower than rates derived from micro-particles in the higher molecular weight colloidal size range (500 nm) and particulate phase (1 and 2 µm) (Fig. 14a and Table 7). However, similar retention efficiency was observed for the colloidal and particulate sized particles as no statistically significant difference was observed ($F = 0.868$, $p = 0.452$). Observed clearance rates were within the ranges of previously observed *in situ* and laboratory-derived rates for quagga mussels (e.g. Baldwin et al. 2002; Bootsma et al. 2012).

Table 4: Average clearance rates (Cl R, in L mussel^{-1} d^{-1}), removal residence times (τ, in h), r^2 values, and p values ± 1 SD determined from exponential decay regressions of microsphere concentrations.

Average ± SD	Microsphere Size					
	20 nm	100 nm	200 nm	500 nm	1 µm	2 µm
Cl R	0.144±0.106	0.017±0.005	0.035±.032	5.80±1.83	8.16±2.91	7.71±4.43
τ	94.1±118.0	312.8±123	216.6±132	0.981±0.591	0.658±0.393	0.0795±0.020
r^2	0.932±0.06	0.117±0.07	0.810±0.15	0.939±0.04	0.942±0.04	0.975±0.48
p	0.0015±0.0019	0.4748±0.14	0.0144±0.012	0.0032±0.0038	0.0044±0.0018	0.0003±0.0004

Interestingly, the 100 nm sized spheres did not display first order removal kinetics (i.e. the p-values of the exponential decay was >0.05) as observed with the 20 nm, 200 nm, 500 nm, 1 µm, and 2 µm sized spheres (Fig. 2b and Table 4) indicating that filtration rate was not related to particle concentration for these specific colloidal sized particles. Particle concentration actually increased between 8 and 24 h suggesting particles may have initially been retained within the gill filaments and slowly released over time as opposed to being egested as pseudofeces effectively removing them from solution. Therefore, clearance rates were calculated differently by dividing the grazing rate over the 24 h incubation (mg h^{-1}) by the concentration of particulate material (mg L^{-1}) to achieve dimensions of L mussel^{-1} h^{-1}. This is a common method of calculating clearance rates (Bootsma et al. 2012) but would be a gross underestimate for 20 and 200 nm

spheres and larger sizes, as the majority of removal took place within the first 2 h (Fig. 14b). Clearance rates determined with 100 and 200 nm particles were lower than with 20 nm particles, although the differences were not significant (all $p>0.05$). This suggests that the space between ctenidial filaments of quagga mussels, or their apparent effective "pore size cutoff", is smaller than 500 nm but larger than 200 nm and the significantly lower retention efficiency of the 20, 100, and 200 nm spheres was largely due to decreased probability of contact with gill filaments and cilia due to the small size of these spherical particles.

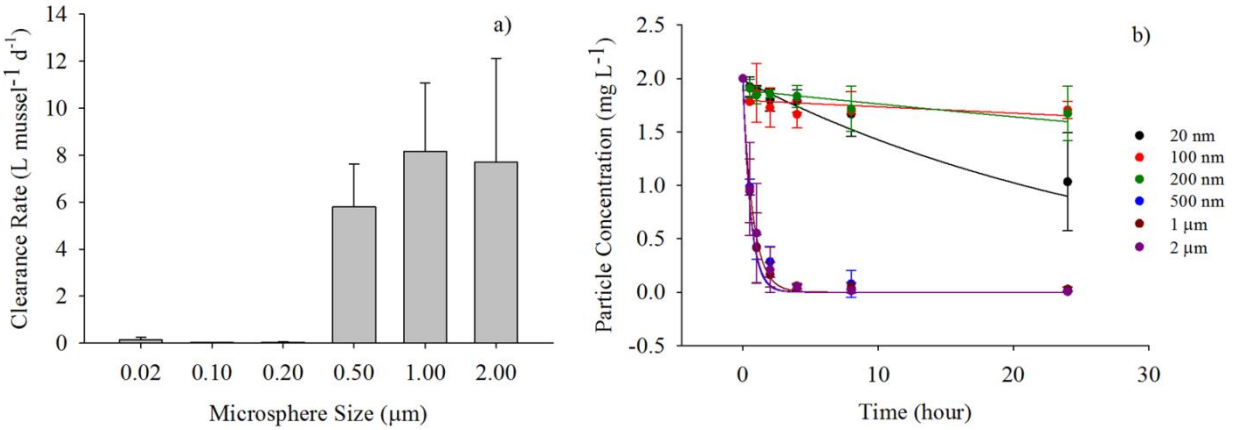

Figure 14: a) Average clearance rates (± 1 SD) of quagga mussels determined with 0.02, 0.1, 0.2 0.5, 1, and 2 µm polystyrene microspheres and b) clearance kinetics of 0.02, 0.1, 0.2, 0.5, 1, and 2 µm microspheres by quagga mussels used to generate clearance rates. Error bars represent 1 standard deviation.

However, it is well known that filter feeding bivalves have the ability to retain particles smaller than the space between ctenidial filaments as a result of the low angle of approach of particles which increases the rate and likelihood of particle contact with filaments, movement of latero-frontal cirri which produce currents that redirect particles towards the frontal surfaces of ctenidial filaments, as well as cilia that extend out from the gills (Jørgensen 1976; Ward et al. 1998). Therefore, it is possible the space between ctenidial filaments is larger than our observed cutoff of 500 nm. For comparison, studies have demonstrated that particle retention efficiency in

zebra mussels (*Dreissena polymorpha*), a congeneric relative of the quagga mussel, began to significantly decrease at particle sizes of 1.5 µm and lower, suggesting that quagga mussels are more efficient than zebra mussels at retaining small material which may further explain their ability to outcompete zebra mussels in Lake Michigan (Jørgensen et al. 1984; Lei et al. 1996).

It is possible that when food or particulate organic matter is sufficient, like the case in laboratory experiments, quagga mussel feeding physiology, such as increased mucus production or increased ciliary and cirri beat rates, are altered to optimize capture rates. When only small (≤200 nm) particles are present, however, mussels may have a more difficult time detecting the presence of food due to decreased contact with gill fibers, so mucus production and ciliary beat rates may not increase resulting in lower capture efficiency as observed. However, there are confounding studies on the plasticity of filter feeding physiology in bivalves (Rosa et al. 2015; Jorgensen 1996 and references therein). Studies have also demonstrated the ability of zebra mussels to directly assimilate DOM (Wang and Guo 2000; Baines et al. 2005, 2007). This is likely the case with quagga mussels in Lake Michigan, especially under conditions with increasing water clarity and decreasing phytoplankton biomass (Cuhel and Aguilar 2013; Binding et al. 2015), however it has yet to be tested. Uptake of DOM has been linked to specific sugar and amino acid carriers, and therefore chemical composition of DOM, and is an active process dependent on external variables such as salinity or sodium concentrations (Baines et al. 2005, Siebers and Winkler 1984). Given that the microspheres used in the present study were inert, uptake would not occur this way and therefore indicates the ability of quagga mussel ctenidial filaments to retain, to a certain degree, DOM and other dissolved materials, regardless of particle quality.

3.4.2 Carbohydrate composition of excreted DOM

As shown in Fig. 15a, the majority of excreted DOM, or 78% of the bulk DOC, consisted of carbohydrates after the 48 h excretion incubation. Within the total dissolved CHO pool, polysaccharides including dilute acid-hydrolysable and dilute acid-resistant PCHO dominated with 60% HR-PCHO and 24% HCl-PCHO (Fig. 15b). Monosaccharides, on the other hand, comprised only 16% of the total dissolved CHO pool suggesting they are more metabolically important or more easily assimilated by quagga mussels. Conversely, PCHO, especially HR-PCHO which are mostly structural CHO, could be difficult to assimilate by quagga mussels due to a lack of endogenous carbohydrases specific to structural PCHO resulting in a high abundance in mussel excreted-DOM.

Carbohydrates have been shown to be the most abundant DOM component in natural waters (e.g. Benner et al. 1992; Hung et al. 2005; Wang et al. 2013; Lin and Guo 2015). Main sources consist of phytoplankton excretion and release from ruptured cells following herbivorous grazing. It seems quagga mussel filtration and excretion may be a source of dissolved carbohydrates, especially polysaccharides, as it facilitates their release from cells of the phytoplankton they graze. This is further supported by the large fraction of carbohydrates comprised of HR-PCHO. Acid-resistant PCHO are thought to be comprised mainly of structural CHO such as cellulose which comprises cell walls of certain phytoplankton like dinoflagellates. Although some studies have reported endogenous cellulase activity in mussels including the zebra mussel indicating their ability to metabolize cellulose, the utilization of cellulose as a carbon source has been observed to be low (<10%) and there are no studies on quagga mussel cellulase or other carbohydrase activity (Langdon and Newell 1990; Palais et al. 2010). This would suggest that a large fraction of ingested cellulose and other structural PCHO are not assimilated and are excreted back into the water column.

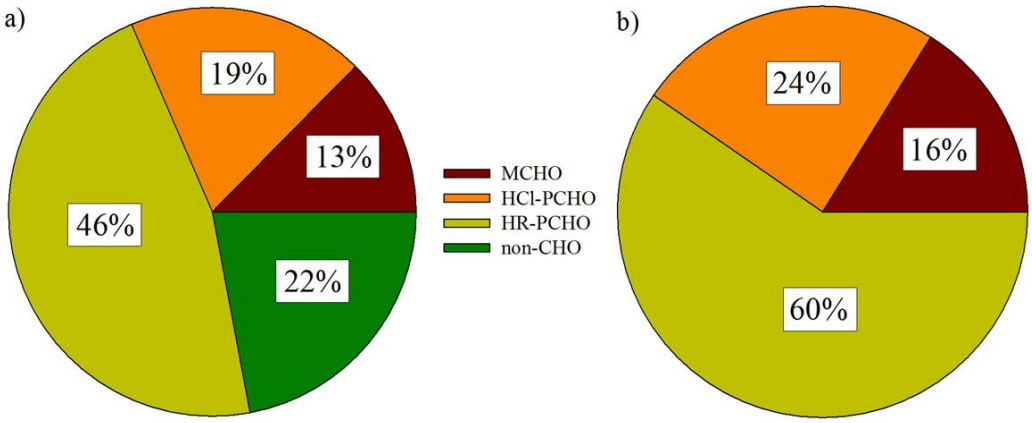

Figure 15: Percent composition of monosaccharides (MCHO), acid-hydrolysable polysaccharides (HCl-PCHO), and diluted HCl-resistant polysaccharides (HR-PCHO) in a) total dissolved carbohydrate pool and b) bulk DOC pool in treatments after 48 h of excretion. Non-CHO represents the fraction of bulk DOC not comprised of carbohydrates.

3.4.3 Chromophoric DOM and optical properties

In addition to bulk DOC, UV-absorbance and derived optical properties including $SUVA_{254}$ and $S_{350-400}$, which are related to DOM aromaticity and molecular weight, respectively, were quantified for the first time to demonstrate the relationship between bulk DOC and optical properties during quagga mussel excretion. Excretion kinetics of CDOM (measured as the absorption coefficient at 254 nm (a_{254})) is depicted in Fig 16a. As shown in Fig. 16b, bulk DOC was significantly correlated to a_{254}. Based on the relationship between DOC and a_{254}, an average non-chromophoric DOC concentration of 13 µM can be estimated for the excreted DOM pool. Although the uncertainties here are large, with the 95% confidence interval ranging from a maximum of 37 to -12 µM, this non-chromophoric DOC comprised only an average of 12% of the bulk DOC pool with a range of 0-34%. In other words, majority of the excreted DOM (with an average of 88%) was chromophoric components. High percentage of chromophotic DOM or low in non-chromophoric DOM components in the quagga mussel excreted DOM is somewhat

surprising since non-chromophoric DOM in river and lake waters is normally below 50% (Zhou et al. 2016) and aquagenic DOM usually has a lower aromaticity compared to terrestrial DOM (e.g. Gueguen et al. 2005). However, model carbohydrates have been shown to contribute to UV absorbance. For example, a 100 µM glucose solution produced an a_{254} value of 0.62 m^{-1}, which was ~20% of the average a_{254} in the experimental beakers after the incubation. Given the high abundance of excreted carbohydrates observed in the present study, it is possible they are responsible for such high chromophoric DOM abundance. Regardless, this suggests the potential of quagga mussel excrement to affect optical properties in the overlying water column.

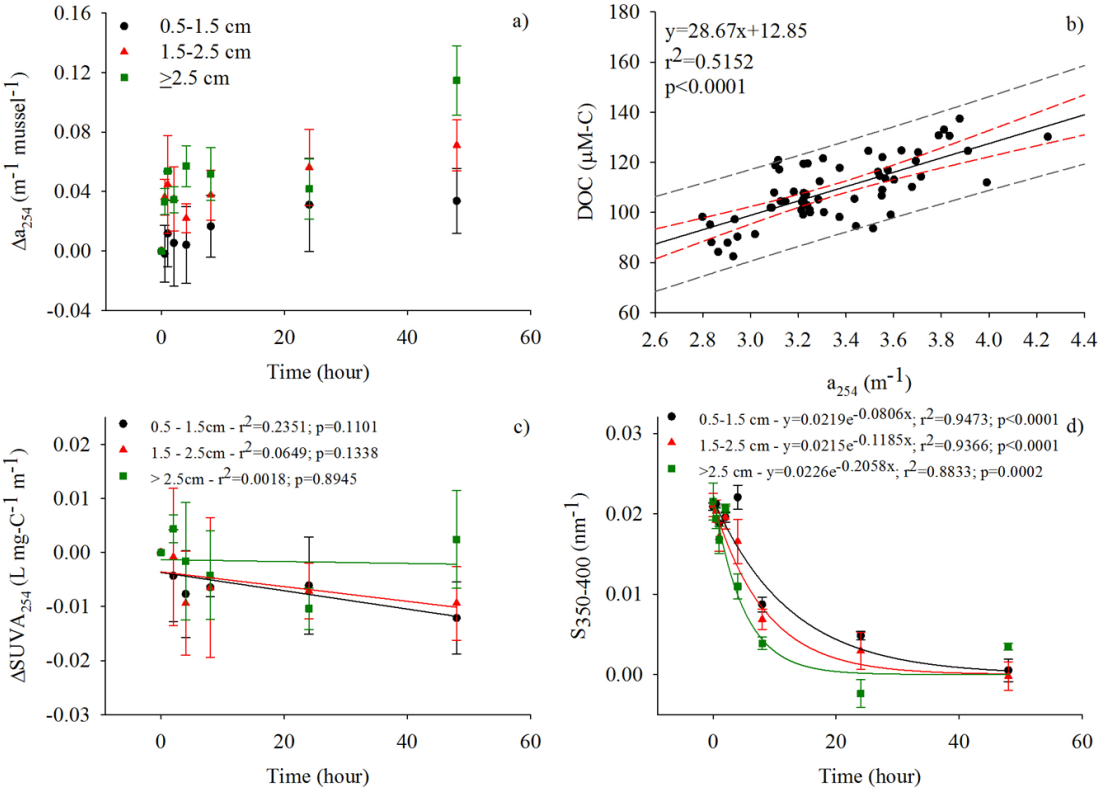

Figure 16: a) Excretion kinetics of CDOM measured as the absorption coefficient at 254 nm (a_{254}), b) the relationship between the absorbance coefficient at 254 nm (a_{254}) and bulk dissolved organic carbon (DOC) (gray dashed lines represent upper and lower limits and red dashed lines represent the 95% confidence interval), c) change in specific UV absorbance at 254 nm ($SUVA_{254}$) over time, and d) change in the spectral slope between 350 and 400 nm ($S_{350-400}$) of excreted DOM.

As seen in Fig. 16c, there was no significant change in the aromaticity of excreted DOM over the course of the incubation. However, spectral slope values decreased during excretion, and the spectral slope-derived DOM molecular weight increased at a similar non-linear rate as bulk DOC excretion (Fig. 16d). This trend indicates that low molecular weight (LMW)-DOM seems to be assimilated preferentially or does not represent a significant fraction of excreted DOM while high molecular weight (HMW)-DOM was consistently being excreted.

3.4.4 Variations in fluorescent DOM components

The fluorescence characteristics of excreted DOM samples are shown in Fig. 17. After 48 h, there was a prominent tryptophan-like peak which has been linked to intact or less degraded, labile peptide material and can be of autochthonous origin as well as from terrestrial and microbial DOM sources (Fellman et al. 2010). Less apparent are peaks A and C, which are both UVC humic-like, commonly linked to terrestrial sources, and are also the major DOM components in lake waters (DeVilbiss et al. 2016; Zhou et al. 2016). This suggests the majority of fluorescent DOM excreted from quagga mussels is of autochthonous origin (i.e. primary production) and is potentially labile. However, proximity to shore and/or anthropogenic influence likely affect the composition of excreted DOM.

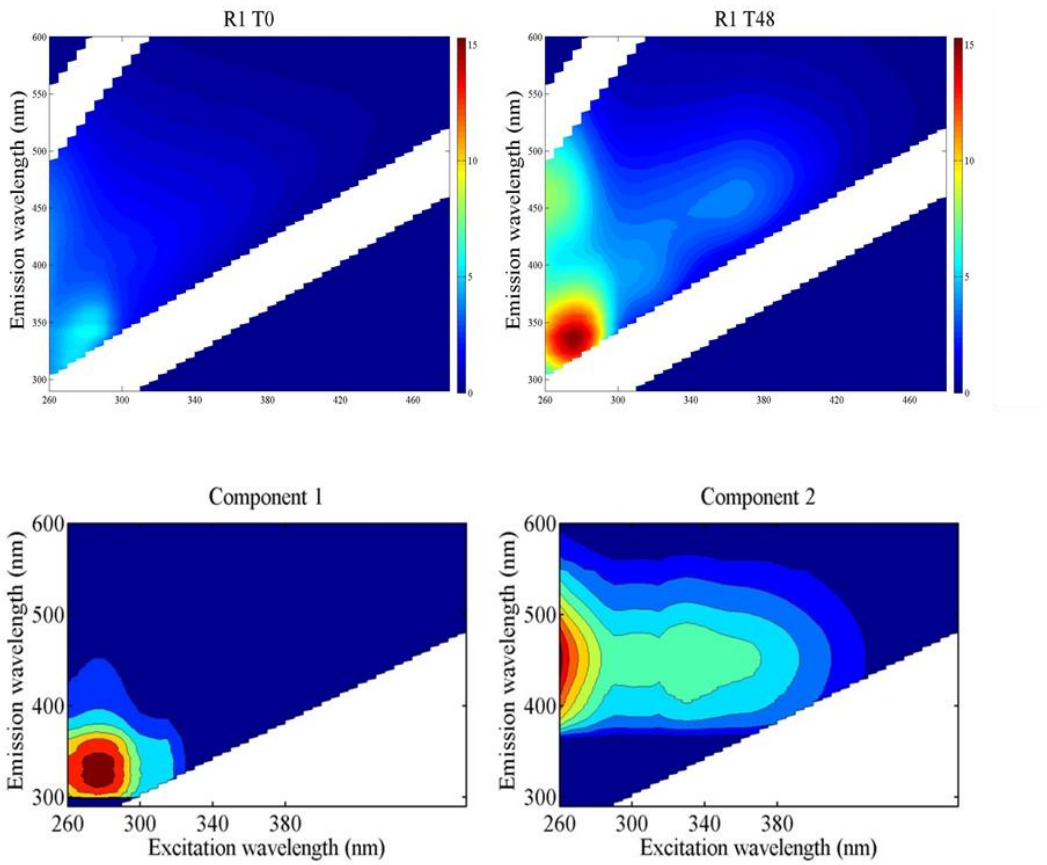

Figure 17: An example of fluorescence EEM spectra from excretion experiments with the 5-15 mm quagga mussels showing the DOM characteristics before excretion (0 h - left panel) and after 48 h of excretion (right panel) and the two PARAFAC-derived components (lower panels). Component 1 Ex/Em = 275/324 nm and component 2 Ex/Em = 260/450 nm. Note the scale is the same for both EEM plots. EEM spectra from all size classes were similar.

PARAFAC analysis was run using EEM data of quagga mussel excrement to generate fluorescent DOM components (Fig. 17). A split-half analysis validated a 2 component model, with the protein-like component, component 1 (C1, peak Ex/Em = 275/324 nm) being the most abundant, followed by humic-like component, component 2 (C2, peak Ex/Em = 260/450 nm). There was no significant trend of C1/C2 over time indicating that while C1 was approximately twice as abundant as C2, the relative abundance of each component did not significantly change over time (Fig 18). There appears to be a slight decrease in C1/C2 ratio between 0 and 8 h, and a slight increase after 8 h, however standard deviations were high. This agrees with the lack of

change in $SUVA_{254}$ values and indicates that, while DOM increased in quantity during excretion, the composition of optically active DOM, both CDOM and FDOM, excreted by mussels remained relatively constant over time.

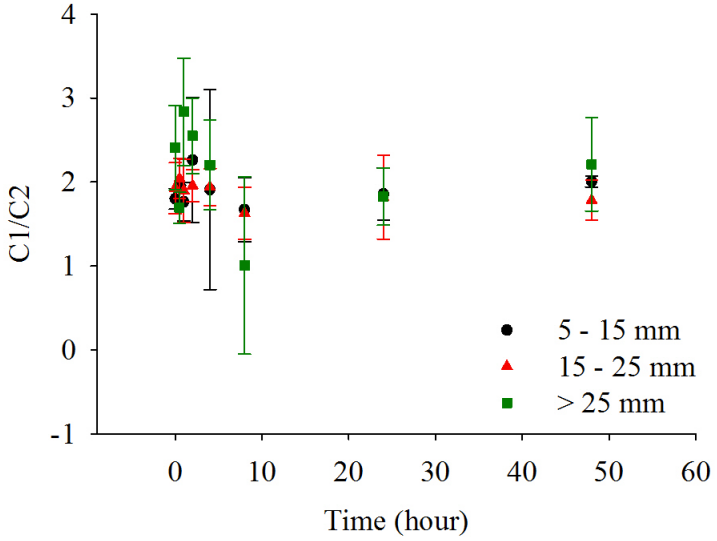

Figure 18: Changes in the ratio of DOM Component 1 to Component 2 (C1/C2) during the incubation.

3.4.5 Size spectra of excreted DOM

The majority of excreted DOM was found to have a colloidal size range of 1 - 5 kDa, including UV-derived chromophoric DOM and fluorescent DOM in humic-like and protein-like components (Fig. 19). In addition to the 1-5 kDa DOM components, chromophoric DOM also contained a significant amount of <1 kDa DOM, likely fulvic acids and lower molecular weight humic acids. Excreted humic-like and protein-like DOM, on the other hand, also contained a significant amount of DOM with a colloidal size between 1-100 kDa (Fig. 19). Collectively, DOM excreted by quagga mussels seems to have a normal size distribution pattern with the 1-5 kDa DOM fraction in the summit. Also, the majority of excreted fluorescent DOM expressed

protein-like fluorescence indicating that it is potentially less degraded and labile which is in agreement with fluorescence EEM data and PARAFAC modeling.

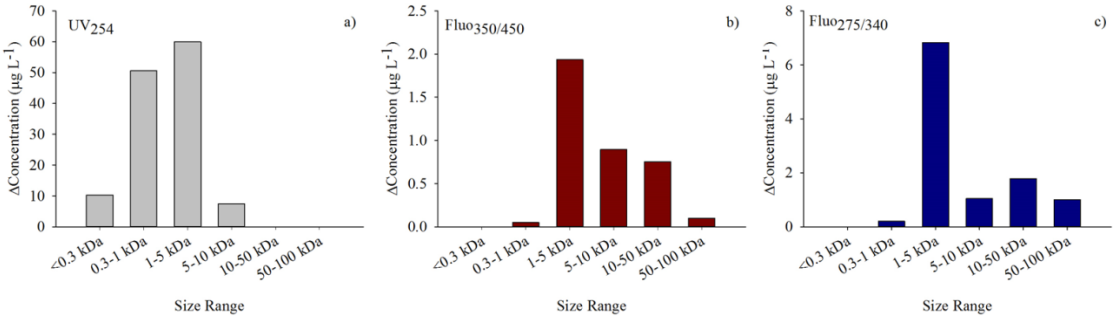

Figure 19: Size distributions of DOM excreted by quagga mussels determined by flow field-flow fractionation techniques showing a) chromophoric DOM derived from UV-absorbance, b) humic-like DOM as quantified by fluorescence Ex/Em of 350/450 nm, and c) protein-like DOM detected by fluorescence Ex/Em=275/340 nm.

3.4.6 Carbon and nutrient (N and P) yields during quagga mussel excretion

Organic carbon species, including bulk DOC and TCHO, displayed non-linear excretion kinetics, with an initial rapid release within the first 4 h followed by a slower, steady rate (Figs. 20a and 20b). On the other hand, nutrient species (i.e. TDN and TDP) remained highly linear over the entire 48 h incubation time (Figs.20c and 20d). It is possible that the sharp initial increase in DOC and TCHO concentrations represents excretion during high food conditions, and once mussels have purged what they filtered and retained from the lake prior to collection, excretion rates decreased representing low food conditions. This would also indicate that the stoichiometry of mussel excrement differs during high and low food conditions, with less OC being excreted compared to nutrients (N and P), perhaps reflecting the metabolic importance of OC during times of low food abundance. However, it is also possible that the steep initial increase in DOC and TCHO concentration is a result of equilibration of interstitial fluid, which should have DOC concentrations similar to lake water which was higher than the ultrafiltered

(<1 kDa) lake water used for the incubation. If this is the case, then the steep initial increase in concentration was a combination of both excretion and interstitial fluid equilibration and the slower rate following 4 h represents a net OC excretion rate.

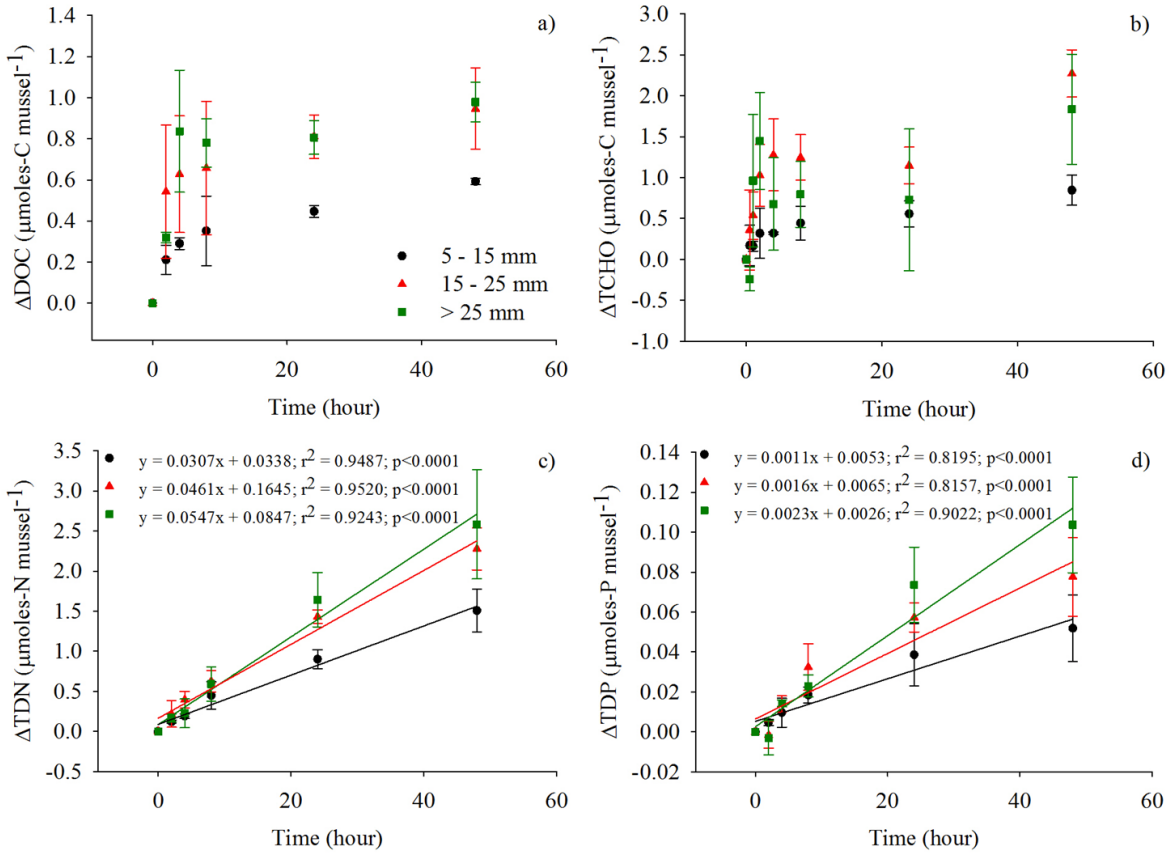

Figure 20: Excretion kinetics of a) dissolved organic carbon (DOC), b) total dissolved carbohydrates (TCHO), c) total dissolved nitrogen (TDN), and d) total dissolved phosphorus, by quagga mussels with three different body size ranges, including the 5-15 mm, 15-25 mm and >25 mm groups. Linear regressions were not shown for DOC and TCHO in order to highlight the non-linear nature of their excretion kinetics.

In order to test this hypothesis, the amount of excess DOC in the interstitial fluid was estimated. 60 µM-C, or the difference in DOC between lake water (150 µM-C) and ultrafiltered water used for the incubation (90 µM-C), and the average length, width, and height for each size class of the mussels was used to calculate their volume, assuming they are rectangular and 10% of the volume was occupied by interstitial fluid. Under these assumptions, between 3.3 and 19

nmoles of DOC could have released into the incubation solution during excretion experiments, which is too small to explain the observed trend. Regardless, the average of the steep initial rate and slower subsequent rate was used when calculating excretion rates. This trend may not have been observed for nutrients because the difference in the concentrations of N and P between lake water and ultrafiltered water are much less than for DOC.

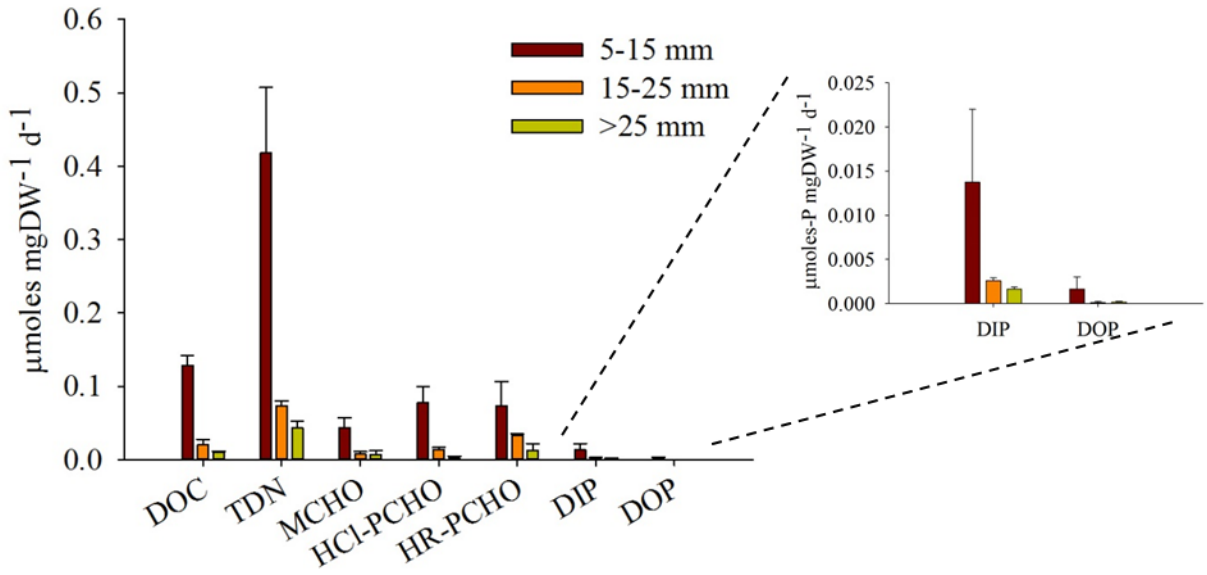

Figure 21: Mass-normalized excretion rates by mussel size class for dissolved organic carbon (DOC), total dissolved nitrogen (TDN), monosaccharides (MCHO), HCl-hydrolysable polysaccharides (HCl-PCHO), diluted HCl-resistant polysaccharides (HR-PCHO), dissolved inorganic phosphorus (DIP), and dissolved organic phosphorus (DOP).

Based on data shown in Fig. 20, mass-normalized excretion rates by different mussel size classes were calculated and are summarized in Table 8 and depicted in Fig. 21 for different carbon and nutrient species including DOC, TDN, MCHO, HCl-PCHO, HR-PCHO, DIP, and DOP. In all measured species, mass-normalized excretion rates decreased with increasing mussel size, with the 5-15 mm class having the highest mass-specific rates, followed by the 15-25 mm class and lastly the >25 mm class. This trend is seemingly contradictory, but similar results have also been reported in other previous studies and indicate that smaller mussels have

higher metabolic rates than larger ones (Tyner et al. 2015; Mosley and Bootsma 2015). Among all measured chemical species, TDN, bulk DOC, and CHO species, including MCHO, HCl-PCHO and HR-PCHO were excreted at the highest rates, with TDN being excreted at a rate 3 times faster than DOC for the smallest size class, while DIP and DOP had the lowest excretion rates (Table 5 and Fig. 21). The excreted DOC/TDN ratios are surprisingly low, averaging 1.1 ± 0.1, whereas the TDN/TDP ratios averaged 32.9 ± 3.8, which is higher than the Redfield ratio but lower than the averaged N/P ratios of lake POM samples (41±13, Peng Lin pers. comm.). Both DOC/TDN and TDN/TDP were significantly lower than the <1 kDa lake water, which averaged 3.3 ± 0.3 and 59.7 ± 7.1, respectively (p<0.0001). Since OC could be metabolized and released in the form of CO_2 while N and P converted from DOM will mostly remain in the solution, a low DOC/TDN ratio suggests that most of the OC being consumed is being metabolized and respired as CO_2.

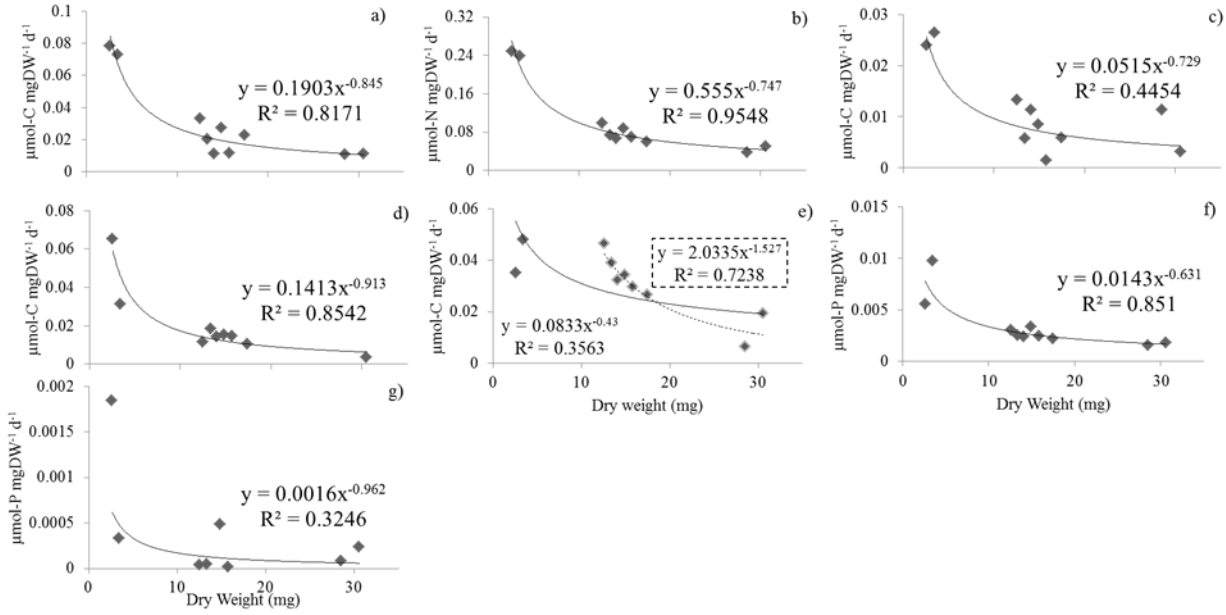

Figure 22: Mass specific excretion rates for a) dissolved organic carbon, b) total dissolved nitrogen, c) monosaccharides, d) HCl-hydrolysable polysaccharides, e) diluted HCl-resistant polysaccharides, f) dissolved inorganic phosphorus, and g) dissolved organic phosphorus. In 3e, the equation surrounded by the dashed lined box corresponds to the dashed regression line, which yielded a much stronger relationship than including the small size class replicates. Both are shown for comparison as they yield significantly different equations and r^2 values

Table 5: Average excretion rates for dissolved organic carbon (DOC), total dissolved nitrogen (TDN), monosaccharides (MCHO), HCl-hydrolysable polysaccharides (HCl-PCHO), diluted HCl-resistant polysaccharides (HR-PCHO), dissolved inorganic phosphorus (DIP), and dissolved organic phosphorus (DOP) (all in µmol $mgDW^{-1}$ day^{-1} ± standard deviation). Average C/N/P ratios were derived from DOC, TDN, and TDP concentrations after 48 h.

Size Class (mm)	DOC	TDN	MCHO	HR-PCHO	HCl-PCHO	DIP	DOP	C/N/P
5-15	0.076 (±0.004)	0.24 (±0.01)	0.025 (±0.002)	0.041 (±0.009)	0.048 (±0.020)	0.0076 (±0.003)	0.0011 (±0.001)	33/33/1
15-25	0.021 (±0.009)	0.076 (±0.010)	0.0077 (±0.004)	0.035 (±0.007)	0.014 (±0.003)	0.0027 (±0.0004)	$9.9x10^{-5}$ (±0.0002)	39/34/1
>25	0.012 (±0.0002)	0.044 (±0.01)	0.0073 (±0.006)	0.013 (±0.029)	0.0018 (±0.003)	0.0017 (±0.0020)	0.00016 (±0.00010)	32/29/1

Mass specific excretion rates followed a power function relationship (Fig. 22) which has been observed in previous studies (Mosley and Bootsma 2015; Bootsma 2009). This highlights the importance of mussel size when inferring the effects of mussel excretion on carbon and nutrient cycling. There have been no reported studies measuring excretion rates of DOC, TDN, and CHO species for comparisons. However, Mosley and Bootsma (2015) reported a DIP mass specific rate of $y = 0.001DW^{-0.343}$ for profundal quagga mussels in Lake Michigan, which is similar to our rate of $y = 0.014DW^{-0.631}$ where DW denotes dry weight in mg.

3.4.7 Organic matter metabolism by quagga mussels

Our results indicate that quagga mussels are highly metabolically efficient, and metabolize the majority of consumed organic matter to CO_2. This is further supported by the discrepancy between capture rate (CR) and settling rate of organic matter. Mosley and Bootsma (2015) determined that the mean areal CR (estimated as the sum of excretion and egestion) of P by quagga mussels was close to 11 times that of the passive settling rate determined by sediment traps indicating quagga mussels recycle a large amount of P to the water column. However, our calculated CR (estimated as the mean areal excretion + egestion rates for the southern basin,

which accounts for mussel size distribution over varying depths, normalized to surface area, m^2) for OC was only 15% of the passive sedimentation rate of carbon reported by Mosley and Bootsma (2015). However, when CR was calculated using excretion rates of DOC and POC per mussel and not per mgDW (dry weight) averaged over the southern basin, the results are significantly different. Assuming a mussel density of 10,000 m^{-2} and applying DOC and POC egestion rates of 0.3 and 1.3 µmol-C $mussel^{-1}$ d^{-1}, respectively, OC-CR was estimated to be 15,700 µmol-C m^{-2} d^{-1}, which is 1.3 times the passive settling rate. The large variability between methods can most likely be attributed to the fact that separate DOC excretion rates were calculated for each size category while only one POC rate was calculated and averaged over the total number of mussels (n = 120) used in all replicates. Regardless, both estimates are significantly less than those observed for P.

This would suggest that while the capture rate of colloids or particles by quagga mussels is higher than the passive settling rate as determined by P estimates, this trend is not observed for OC because the vast majority of captured organic matter is metabolized and respired as CO_2, which was not measured in our incubation experiments. However, the vast majority of TDP, including organic and inorganic dissolved P, is excreted or egested and remains in solution with minimal amounts being allocated to growth and reproduction (Stoeckmann and Garton 1997). These findings also support the high observed TDN excretion rates, which is likely comprised predominately of ammonia, a metabolic byproduct (Stoeckmann and Garton 1997). Stoeckmann and Garton (1997) also determined that metabolism comprises >90% of zebra mussels energy budget. Further, ^{14}C tracer studies showed that a significant amount of DOC consumed by zebra mussels was respired as CO_2, and therefore must have been metabolized (Baines et al. 2005), all in support of our findings.

3.4.8 Implications for water column biogeochemistry in southern Lake Michigan

In order to gauge the importance of mussel grazing, metabolism, and excretion/egestion in Lake Michigan, mass specific DOC excretion rates (Table 8) for each mussel size class were used to estimate annual DOC excretion in the southern basin of Lake Michigan. Specifically, mussel densities and size distributions divided into depth classes of 0-15 m, 16-30 m, 31-50 m, 51-90 m, and >90 m reported in Nalepa et al. (2010) and summarized in Table 6 were used to generate areal DOC fluxes (in µmoles-C m^{-2} d^{-1}) which were then integrated across the southern basin of Lake Michigan and extrapolated to one year (Tyner et al. 2015). Excretion of DOC was estimated at $5.9x10^7$ kg-C yr^{-1} in the southern basin, which only accounts for ~4% of total OC consumption in southern Lake Michigan estimated using dissolved O_2 consumption (Tyner et al. 2015). This indicates that 96% of consumed OC is either respired as CO_2, egested as feces/pseudofeces, converted to biomass, or allocated to reproduction, all indicating a loss of OC to the water column. A rough estimate of POC egestion indicates only 8% ($1.0x10^4$ kg-C yr^{-1}) of consumed organic matter is egested. This suggests the majority is respired as CO_2, supporting observed high assimilation efficiencies which have been suggested as a reason allowing the persistence of quagga mussels under low food conditions like open Lake Michigan (Cuhel and Aguilar 2013). However, POC egestion rates were normalized over the average mass of all mussel size classes because egestion rates were not measured separately for each size class. Regardless, these results indicate quagga mussels are a massive sink for OC but a source for CO_2 in Lake Michigan.

The high assimilation efficiency of OC and the release of CO_2 by benthic quagga mussels observed here are consistent with changes in CO_2 dynamics in Lake Michigan after the colonization of invasive mussels. For example, over the last decade, the partial pressure of CO_2

(pCO_2) in the water column has been increasing in the Great Lakes, especially in Lake Michigan (Peng Lin, Pers. comm.). This has been attributed to the introduction of quagga mussels in the Great Lakes. Thus, invasive quagga mussels could have changed carbon dynamics in the water column through metabolizing and respiring the vast majority of their OC intake.

Table 6: Density and size distribution of quagga mussels at different depth intervals in Lake Michigan and total lake bottom area for each depth class for the southern basin of Lake Michigan. Data summarized from Nalepa et al. (2010).

Depth (m)	Total Area (m^2)	No. of mussels in different size classes			
		0-15 mm	15-25 mm	>25 mm	Total
0-15	$1.84x10^8$	458	4,250	58	4,766
16-30	$3.98x10^9$	8,680	70	0	8,750
31-50	$2.04x10^9$	6,016	1,920	64	8,000
51-90	$5.67x10^9$	14,640	345	15	15,000
>90	$5.91x10^9$	4,428	14	18	4,459

3.5 Conclusion

Invasive quagga mussels appear to have the ability to physically retain smaller dissolved and colloidal particles than zebra mussels. The composition of excreted DOM consisted mainly of carbohydrates, specifically structural polysaccharides, suggesting quagga mussels could have altered the composition of the DOM pool in Lake Michigan by selectively retaining and metabolizing fractions of DOM. The excreted DOM also displayed chromophoric and fluorescent properties with protein-like DOM being the major fluorescent-DOM component, suggesting they are susceptible to photodegradation or highly reactivite. The lack of change in aromaticity and the ratio of PARAFAC-derived DOM components over time indicated that while the abundance of CDOM and FDOM increased over time, the composition or quality did not change significantly. Spectral slope and size distribution data indicated that the bulk of excreted DOM had typical size spectra centralized at 1-5 kDa. In addition, the excreted DOM seemed mostly HWM-DOM with less LMW-DOM. High excretion rates of TDN compared to DOC,

along with the discrepancy between the capture rate of DOC and P suggest that quagga mussels have high assimilation efficiencies and respire most consumed OC to CO_2. During incubation, only ~12% of consumed OC is excreted as DOC and egested as POC, with the majority of OC is being converted to CO_2.

4. References

Achman, D. 1993. Volatilization of polychlorinated biphenyls from Green Bay, Lake Michigan. Environ. Sci. Technol. 27: 75-87.

Amon, R, and Benner, R. 1996. Photochemical and microbial consumption of dissolved organic carbon and dissolved oxygen in the Amazon River system. Geochim. Cosmochin. Acta. 60: 1783-1792.

Amon, R. and Benner, R. 1996. Bacterial utilization of different size classes of dissolved organic matter. Limnol. Oceanogr. 41: 41–51.

Ankley, G. T., Lodge, K., Call, D. J., Balcer, M. D., Brooke, L. T., Cook, P. M., Kreis Jr., R. G., Carlson , and others. 1992. Integrated assessment of contaminated sediments in the lower fox river and green bay, Wisconsin. Ecotoxicol. Environ. Saf. 23: 46–63.

Baalousha, M., Stolpe, B., and Lead, J. 2011. Flow field-flow fractionation for the analysis and characterization of natural colloids and manufactured nanoparticles in environmental systems: a critical review. Journal Chromatogr. A. 1218: 4078–103.

Baines, S., Fisher, N., and Cole, J. 2007. Dissolved organic matter and persistence of the invasive zebra mussel (Dreissena polymorpha) under low food conditions. Limnol. Oceanogr. 52: 70–78.

Baines, S., Fisher, N., and Cole, J. 2005. Uptake of dissolved organic matter (DOM) and its importance to metabolic requirements of the zebra mussel, Dreissena polymorpha. Limnol. Oceanogr. 50: 36–47.

Baldwin, B. S., Mayer, M. S., Dayton, J., Pau, N., Mendilla, J., Sullivan, M., Moore, A., Ma, A., and Mills, E. L. 2002. Comparative growth and feeding in zebra and quagga mussels (Dreissena polymorpha and Dreissena bugensis): implications for North American lakes. Can. J. Fish. Aquat. Sci. 59: 680–694.

Bauer, J. E., and Bianchi, T. S. 2011. Dissolved organic carbon cycling and transformation. Treatise on Estuarine and Coastal Science. 5: 7–68, doi: 10.1016/B978-0-12-374711-2.00502-7.

Belzile, C., Vincent, W. F., and Kumagai, M. 2002. Contribution of absorption and scattering to the attenuation of UV and photosynthetically available radiation in Lake Biwa. Limnol. Oceanogr. 47: 95–107.

Benner, R., Pakulski, J. D., McCarthy, M., Hedges, J. I., and Hatcher, P. G. 1992. Bulk chemical characteristics of dissolved organic matter in the ocean. Science. 255: 1561-1564.

Benner, R., and Amon, R. M. 2015. The size-reactivity continuum of major bioelements in the ocean. Annu. Rev. Mar. Sci. *7*: 2.1-2.21.

Bianchi, T. S., DiMarco, S. F., Cowan, J. H., Hetland, R. D., Chapman, P., Day, J. W. and Allison, M. A., 2010. The science of hypoxia in the Northern Gulf of Mexico: a review. Sci. Total Environ. 408: 1471-1484.

Biddanda, B. A. and Cotner, J. B. 2002. Love Handles in Aquatic Ecosystems: The Role of Dissolved Organic Carbon Drawdown, Resuspended Sediments, and Terrigenous Inputs in the Carbon Balance of Lake Michigan. Ecosystems. 5: 431–445.

Binding C. E., Greenberg, T. A., Watson, S. B., Rastin, S. and Gould, J. 2015. Long term water clarity changes in North America's Great Lakes from multi-sensor satellite observations. Limnol. Oceanogr. 60: 1976-1995.

Bootsma, H., 2009. Causes, consequences and management of nuisance cladophora. US Enviromental Protection Agency Project GL-00E06901.

Bootsma, H., Waples, J. T., and Liao, Q. 2012. Identifying major phosphorus pathways in the Lake Michigan nearshore zone. MMSD Contract M03029P05, Milwaukee Metropolitan Sewerage District, Milwaukee, WI.

Bunnell, D.B., Madenjian, C. P., and Claramunt, R. M. 2006. Long-term changes of the Lake Michigan fish community following the reduction of exotic alewife (Alosa pseudoharengus). Can. J. Fish. Aquat. Sci. 63: 2434–2446.

Chari, N. V. H. K., Rao, P., and Sarma, N. 2013. Fluorescent dissolved organic matter in the continental shelf waters of western Bay of Bengal. J. Earth Syst. Sci. 122: 1325–1334.

Chari, N. V. H. K., Sarma, N. S., Pandi, R. S., and Murthy, N. K. 2012. Seasonal and spatial constraints of fluorophores in the midwestern Bay of Bengal by PARAFAC analysis of excitation emission matrix spectra. Estuar. Coast. Shelf. S. 100: 162–171.

Coble, P. G. 2007. Marine optical biogeochemistry: the chemistry of ocean color. Chem. Rev. 107: 402–18.

Cole, J. J., Prairie, Y. T., Caraco, N. F., McDowell, W. H., Tranvik, L. J., Striegl, R. G., Duarte, C. M., Kortelainen, P, and others. 2007. Plumbing the global carbon cycle: integrating inland waters into the terrestrial carbon budget. Ecosystems 10: 172-185. doi:110.1007/s10021-10006-19013-10028.

Conroy, J. D., Edwards, W. J., Pontius, R. A., Kane, D. D., Zhang, H., Shea, J. F., Richey, J. N., and Culver, D. A. 2005. Soluble nitrogen and phosphorus excretion of exotic freshwater mussels (Dreissena spp.): potential impacts for nutrient remineralisation in western Lake Erie. Freshwater Biol. 50: 1146–1162.

Cory, R. M., and McKnight, D. M. 2005. Fluorescence spectroscopy reveals ubiquitous presence of oxidized and reduced quinones in dissolved organic matter. Environ. Sci. Technol. 39:

8142–8149.

Crawford, C. C., Hobbie, J. E., and Webb, K.. L. 1974. The utilization of dissolved free amino acids by estuarine microorganisms. Ecology. 55: 551-563.

Cuhel, R. L., and Aguilar, C. 2013. Ecosystem transformations of the Laurentian Great Lake Michigan by nonindigenous biological invaders. Annu. Rev. Mar. Sci. 5: 289–320.

De Leeuw, J. W. and Largeau, C. 2003. A review of macromolecular organic compounds that comprise living organisms and their role in kerogen, coal, and petroleum formation. M.H. Engel, S.A. Macko (Eds.), Organic Geochemistry, Springer, USA. 23-72.

De Stasio, B., Schrimpf, M., and Cornwell, B. 2014. Phytoplankton communities in Green Bay, Lake Michigan after invasion by Dreissenid Mussels: increased dominance by cyanobacteria. Diversity. 6: 681–704.

Diaz, R. J., and Rosenberg, R. 2008. Spreading dead zones and consequences for marine ecosystems. Science 321: 926–929.

Diffey, B. L. 2002. Sources and measurement of ultraviolet radiation. Methods: 4–13.

Eadie, B. J., Klump, J. V., Landrum, P. F. 1992. Distribution of hydrophobic organic compounds between dissolved and particulate organic matter in Green Bay waters. J. Great Lakes Res. 18: 91–97.

Egan, D. 2008. Ecological problem, economic distress. Milwaukee J. Sentin. June 30. http://www.jsonline.com/news.wisconsin/29571999.html.

Egan, D. 2014. Dead zones haunt Green Bay as manure fuels algae blooms. Milwaukee J. Sentin., Sept 30. http://www.jsonline.com/news/wisconsin/dead-zones-haunt-green-bay-as-manure-fuels-algae-blooms-die-offs-b99344902z1-274684741.html

Fellman, J. B., Hood, E., and Spencer, R. G. M. 2010. Fluorescence spectroscopy opens new windows into dissolved organic matter dynamics in freshwater ecosystems: a review. Limnol. Oceanogr. 55: 2452-2462.

Giddings, J. C. 1993. Field-flow fractionation: analysis of macromolecular, colloidal, and particulate materials. Science. 260: 1456–65.

Green, R. E., Bianchi, T. S., Dagg, M. J., Walker, N. D., and Breed, G. A. 2006. An organic carbon budget for the Mississippi River turbidity plume and plume contributions to air-sea CO2 fluxes and bottom water hypoxia. Estuar. Coast. 29: 579–597.

Guéguen, C., Granskog, M. A., McCullough, G., and Barber, D. G. 2011. Characterisation of colored dissolved organic matter in Hudson Bay and Hudson Strait using parallel factor analysis. J. Marine. Syst. 88: 423–433.

Guo, L., Santschi, P. H., and Warnken, K. W. 1995. Dynamics of dissolved organic carbon (DOC) in oceanic environments. Limnol. Oceanogr. 40: 1392–1403.

Guo, L., and Santschi, P. H. 1997. Measurements of dissolved organic carbon (DOC) in sea water by high temperature combustion method. Atca. Oceanol. Sin. 16: 339–353.

Guo, L., Hunt, B. J., Santschi, P. H., and Ray, S. M. 2001. Effects of dissolved organic matter on the uptake of trace metals by American oysters. Environ. Sci. Technol. 35: 885-893

Guo, L., P. H. Santschi, and S. Ray. 2002. Metal partitioning between colloidal and dissolved phases and its relation with bioavailability to American oysters. Mar. Environ. Res. 54: 49-64.

Guo, L., Ping, C., and Macdonald, R. W. 2007. Mobilization pathways of organic carbon from permafrost to arctic rivers in a changing climate. Geophys. Res. Lett. 34: 1-5

Guo, L. and P. H. Santschi. 2007. Ultrafiltration and its applications to sampling and characterisation of aquatic colloids. In: Wilkinson, K. J. and Lead, J. R. Eds., Environmental colloids and particles, IUPAC Series on Analytical and Physical Chemistry of Environmental Systems, John Wiley.

Gustafsson, Ö. and Gschwend, P. M., 1997. Aquatic colloids: Concepts, definitions, and current challenges. Limnol. Oceanogr. 42(3), pp.519–528.

Hamidi, S. A., Bravo, H., Klump, J. V., and Waples, J. T. 2015. The role of circulation and heat fluxes in the formation of stratification leading to hypoxia in Green Bay, Lake Michigan, J. Great Lakes Res., dx.doi.org/10.1016/j.jglr.2015.08.007

Harris, V. A., and Christie, J. 1987. The lower Green Bay remedial action plan: nutrient and eutrophication management, Technical Advirsory Committee report. Publication no. WR-167-87. Wisconsin Department of Natural Resources, Madison, Wis.

Haye, J., Santschi, P. H., Roberts, K. A., and Ray, S. 2006. Protective role of alginic acid against metal uptake by American oyster (Crassostrea virginica). Environ. Chem. 3: 172-183.

Hecky, R. E., Smith, R. E. H., Barton, D. R., Guildford, S. J., Taylor, W. D., Charlton, M. N., and Howell, T. 2004. The nearshore phosphorus shunt: a consequence of ecosystem engineering by dreissenids in the Laurentian Great Lakes. Can. J. Fish. Aquat. Sci. 61: 1285-1293.

Hedges, J. I., and Keil, R. G. 1995. Sedimentary organic matter preservation: an assesment and speculative synthesis. Mar. Chem. 49: 137-139.

Hedges, J. I., Keil, R. G., and Benner, R. 1997. What happens to terrestrial organic matter in the ocean? Org. Geochem. 27: 195-212

Helms, J. R., Stubbins, A., Ritchie, J. D., Minor, E. C. 2008. Absorption spectral slopes and slope ratios as indicators of molecular weight, source, and photobleaching of chromophoric dissolved organic matter. Limnol. Oceanogr. 53: 955–969.

Herdendorf, C. E. 1990. Great Lakes Estuaries. Estuaries. 13: 493–503.

Holmes, R. M., McClelland, J. W., Raymond, P. A., Frazer, B. B., Peterson, B. J., and Stieglitz, M. 2008. Labilty of DOC transported by Alaskan rivers to the Arctic Ocean. Geophys. Res. Lett. 35: 1-5.

Honeyman, B. D., and Santschi, P. H. 1992. The role of particles and colloids in the transport of radionuclides and trace metals in the ocean. In: Buffle, J., van Leeuwen, H.P. (Eds), Environmental Particles. Lewis Publishers, Chelsea, MI.

Hung, C. C., Tang, D., Warnken, K. W., and Santschi, P. H. 2001. Distributions of carbohydrates, including uronic acids, in estuarine waters of Galveston Bay. *Mar. Chem. 73*(3): 305-318

Ishii, S., and Boyer, T. 2012. Behavior of reoccurring PARAFAC components in fluorescent dissolved organic matter in natural and engineered systems: a critical review. Environ. Sci. Technol. 46: 2006-2017.

Jørgensen, C., Kiørboe, T., Møhlenberg, F., and Riisgard, H. U. 1984. Ciliary and mucus-net filter feeding, with special reference to fluid mechanical characteristics. Mar. Ecol. Prog. Ser. 15: 283–292.

Jorgensen, C. B. 1996. Bivalve filter feeding revisited. Mar. Ecol. Prog. Ser. 142: 287–302.

Kepkay, P. E., Niven, S. E. H., and Milligan, T. G. 1993. Low molecular weight and colloidal DOC production during a phytoplankton bloom. Mar. Ecol. Prog. Ser. 100: 233-244.

Kerfoot, W. C., Yousef, F., Green, S. A., Budd, W. J., Schwab, D. J., and Vanderploeg H. A. 2010. Approaching storm: Disappearing winter bloom in Lake Michigan. J. Great Lakes Res. 36: 30–41.

Kieber, D. J., McDaniel, J., and Mopper, K. 1989. Photochemical source of biological substrates in sea water: implications for carbon cycling. Nature. 341: 31-69.

Kieber, R. J., Hydro, L. H., Seaton, P. J. 1997. Photooxidation of triglycerides and fatty acids in seawater: implications toward the formation of marine humic substances. Limnol. Oceanogr. 42: 1454-1462.

Klump, J. V., Edgington, D. N., Sager, P. E., and Robertson, D.M. 1997. Sedimentary phosphorus cycling and a phosphorus mass balance for the Green Bay (Lake Michigan) ecosystem. Can. J. Fish. Aquat. Sci. 54: 10–26.

Klump, J. V., Fitzgerald, S. A., and Waples, J. T. 2009. Benthic biogeochemical cycling, nutrient stoichiometry, and carbon and nitrogen mass balances in a eutrophic freshwater bay. Limnol. Oceanogr. 54: 692–712.

Langdon, C., and Newell, R. 1990. Utilization of detritus and bacteria as food sources by two bivalve suspension-feeders, the oyster Crassostrea virginica and the mussel Geukensia demissa. Mar. Ecol. Prog. Ser. 58: 299–310.

Lathrop, R. G., Vande Castle, J. R., and Lillesand, T. M. 1990. Monitoring river plume transport and mesoscale circulation in Green Bay, Lake Michigan, through satellite remote sensing. J. Great. Lakes. Res. 16: 471–484.

Leenheer, J. A., and Croué, J. 2003. Characterizing aquatic dissolved organic matter. *Environ. Sci. Technol., 37*(1): 18A-26A.

Lei, J., Payne, B. S., and Wang, S. Y. 1996. Filtration dynamics of the zebra mussel, Dreissena polymorpha. Can. J. Fish. Aquat. Sci. 53: 29–37.

Lennon, J. T., and Pfaff, L. E.. 2005. Source and supply of terrestrial organic matter affects aquatic microbial metabolism. Aquat. Microb. Ecol. 39: 107-119.

Lin, P. and Guo, L. 2015. Spatial and vertical variations of dissolved carbohydrates in the northern Gulf of Mexico following the Deepwater Horizon oil spill. Mar. Chem. 174: 13-25, doi: 10.1016/j.marchem.2015.04.001

Lin, P., Klump, J. V. and Guo, L. 2016. Dynamics of dissolved and particulate phosphorus influenced by seasonal hypoxia in Green Bay, Lake Michigan. *Science of The Total Environment*, 541: 1070-1082.

Loder, T. C., and Reichard, R. P. 1981. The dynamics of conservative mixing in estuaries. Estuaries. 4: 64-69.

Markager, S., Stedmon, C. A., and Søndergaard, M. 2011. Seasonal dynamics and conservative mixing of dissolved organic matter in the temperate eutrophic estuary Horsens Fjord. Estuar. Coast. Shelf. S. 92: 376-388.

Martin, S. C., Hinz, S. C., Rodgers, P. W., Bierman Jr., V. J., DePinto, J. V., and Young, T. C. 1995. Calibration of a hydraulic transport model for Green Bay, Lake Michigan. J. Great. Lakes. Res. 21: 599–609.

Matsuoka, A., Bricaud, A., Benner, R., Para, J., Sempére, R., Prieur, L., Bélanger, S., and Babin, M. 2012. Tracing the transport of colored dissolved organic matter in water masses of the Southern Beaufort Sea: relationship with hydrographic characteristics. Biogeosciences, 9: 925–940.

McCarthy, J., and Zachara, J. 1989. Subsurface transport of contaminants. Environ. Sci. Technol. 23: 496–502.

McGuire, D. A., Anders, L. G., Christensen, T. R., Dallimore, S., Guo, L., Hayes, D. J., Heimann, M., Lorenson, T. D., and others. 2009. Sensitivity of the carbon cycle in the Arctic to climate change. Ecol. Monogr. 79: 523-555.

McKnight, D. M., Boyer, E. W., Westerhoff, P. K., Doran, P. T., Kulbe, T., and Anderson, D. T. 2001. Spectrofluorometric characterization of dissolved organic matter for indication of precursor organic material and aromaticity. Limnol. Oceanogr. 46: 38–48.

Miller, W.L., and Zepp, R. G. 1995. Photochemical production of dissolved inorganic carbon from terrestrial organic matter: significance to the oceanic organic carbon cycle. Geophys. Res. Lett. 22: 417-420.

Miller, W. L., and Moran, M. A. 1997. Interaction of photochemical and microbial processes in the degradation of refractory dissolved organic matter from a coastal marine environment. Limnol. Oceanogr. 42: 1317–1324.

Modlin, R. F., and Beeton, A. M. 1970. Dispersal of Fox River water in Green Bay, Lake Michigan. Proceedings of the 13th Conference of Great Lakes Research.

Møller, E. V., Thor, P., and Nielsen, T. G. 2003. Production of OC by *Calanus finmarchicus*, *C. glacialis* and *C. hyperboreus* through sloppy feeding and leakage from fecal pellets. 2003. Mar. Ecol. Prog. Ser. 262: 185-191.

Møller, E. F. 2007. Production of dissolved organic carbon by sloppy feeding in the copepods *Acartia tonsa*, *Centropages typicus*, and *Temora longicornis*. Limnol. Oceangr. 53: 79-84

Moran, M. A., Sheldon, W. M., and Zepp, R. G. 2000. Carbon loss and optical property changes during long-term photochemical and biological degradation of estuarine dissolved organic matter. Limnol. Oceanogr. 45: 1254–1264.

Mortimer, C. H. 1978. Water movement, mixing, and transport in Green Bay, Lake Michigan. Univ. Wisconsin Sea Grant Institute No. WI-SG-78-234.

Mosley, C., and Bootsma, H. 2015. Phosphorus recycling by profunda quagga mussels (Dreissena rostriformis bugensis) in Lake Michigan. J. Great Lakes Res. 41: 38-48.

Nalepa, T. F., Fanslow, D. L., and Pothoven S. A. 2010. Recent changes in density, biomass, recruitment, size structure, and nutritional state of Dreissena populations in southern Lake Michigan. J. Great Lakes Res. 36: 5–19.

O'loughlin, E. J., and Chin, Y. 2009. Quantification and characterization of dissolved organic carbon and iron in sedimentary porewater from Green Bay, WI, USA. Biogeochemistry. 71: 371–386.

Ohno, T. 2002. Fluorescence inner-filtering correction for determining the humification index of dissolved organic matter. Environ. Sci. Technol. 36: 742–746.

Parlanti, E., Wörz, K., and Lamotte, G. M. 2000. Dissolved organic matter fluorescence spectroscopy as a tool to estimate biological activity in a coastal zone submitted to anthropogenic inputs. Org. Geochem. 31: 1765–1781.

Qualls, T. M., Dolan, D. M., Reed. T., Zorn, M. E., and Kennedy, J. 2007. Analysis of the impacts of the zebra mussel, Dreissena polymorpha, on nutrients, water clarity, and the chlorophyll-phosphorus relationship in Lower Green Bay. J. Great Lakes. Res. 33: 617–626.

Ramcharan, C., and C. B. Turner. 2010. Influence of zebra (Dreissena polymorpha) and quagga (Dreissena rostriformis) mussel invasions on benthic nutrient and oxygen dynamics. Can. J. Fish. Aquat. Sci. 67: 1899–1908.

Ravichandran, M. 2004. Interactions between mercury and dissolved organic matter - a review. Chemosphere. 55: 319-331.

Rochelle-Newall, E., and Fisher, T. 2002. Chromophoric dissolved organic matter and dissolved organic carbon in Chesapeake Bay. Mar. Chem. 77: 23–41.

Rosa, M., Ward, J. E., Ouvrard, M., Holohan, B. A., Espinosa, E. P., Shumway, S. E., and Allam, B. 2015. Examining the physiological plasticity of particle capture by the blue mussel, Mytilus edulis (L.): Confounding factors and potential artifacts with studies utilizing natural seston. J. Exp. Mar. Biol. Ecol. 473: 207–217.

Santschi, P. H., Guo, L., Means, J. C. and Ravichandran, M. 1999. Natural organic matter binding of trace metals and trace organic contaminants in estuaries. Biogeochemistry of Gulf of Mexico Estuaries, pp.347-380, Wiley.

Schindler, D. E., and M. D. Scheuerell. 2002. Habitat coupling in lake ecosystems. Oikos, 98: 177–189.

Smith, P. L., Ragotzkie, R. A., Andren, A. W., Harris, H. J. 1988. Estuary rehabilitation: the Green Bay story. Oceanus. 31: 12–20.

Søndergaard, M., Hansen, B., and Markager, S. 1995. Dynamics of dissolved organic carbon lability in a eutrophic lake. Limnol. Oceanogr. 40: 46-54.

Stedmon, C. A., Markager, S. and Kaas, H., 2000. Optical properties and signatures of chromophoric dissolved organic matter (CDOM) in Danish coastal waters. Estuar. Coast. Shelf. S. 51: 267–278.

Stedmon, C. A. and Markager, S. 2003. Behaviour of the optical properties of coloured dissolved organic matter under conservative mixing. Estuar. Coast. Shelf. Sci. 57: 1-7.

Stedmon, C. A., and Markager, S. 2005. Resolving the variability in dissolved organic matter fluorescence in a temperate estuary and its catchment using PARAFAC analysis. Limnol. Oceanogr. 50: 686–697.

Stedmon, C. A., and Bro, R. 2008. Characterizing dissolved organic matter fluorescence with parallel factor analysis: a tutorial. Limnol. Oceanogr. Methods. 6: 572-579.

Siegel, D. A. and Michaels, A. F. 1996. Quantification of non-algal light attenuation in the Sargasso Sea: implications for biogeochemistry and remote sensing. Deep-sea research II. 43: 321-345

Stoeckmann, A. M., and Garton, D. W. 1997. A seasonal energy budget for zebra mussels (Dreissena polymorpha) in western Lake Erie. Can. J. Fish. Aquat. Sci. 54: 2743–2751.

Stolpe, B., Guo, L., Shiller, A. M., and Hassellöv, M. 2010. Size and composition of colloidal organic matter and trace elements in the Mississippi River, Pearl River and the northern Gulf of Mexico, as characterized by flow field-flow fractionation. Mar. Chem. 118: 119–128.

Thomas, J. D. 1997. The role of dissolved organic matter, particularly free amino acids and humic substances, in freshwater ecosystems. Freshwater Biol. 38: 1-36.

Tyner, E. H., Bootsma, H. A., and Moraska, B. 2015. Dreissenid metabolism and ecosystem-scale effects as revealed by oxygen consumption. J. Great Lakes Res. DOI: http://dx.doi.org/10.1016/j.jglr.2015.05.009.

Uher, G., Hughes, C., Henry, G., and Upstill-Goddard, R.C. 2001. Non-conservative mixing behavior of colored dissolved organic matter in a humic-rich, turbid estuary. Geophys. Res. Lett. 28: 3309-3312.

Vanderploeg, H. A., Liebig, J. R., Nalepa, T. F., Fahnenstiel, G. L., and Pothoven, S. A. 2010. Dreissena and the disappearance of the spring phytoplankton bloom in Lake Michigan. J. Great Lakes Res. 36: 50–59.

Voelker, B. M., Morel, F. M. M., and Sulzberger, B. 1997. Iron redox cycling in surface waters: effects of humic substances and light. Environ. Sci. Technol. 31: 1004-1011.

Vonk, J. E., Sánchez-Garcia, L., von Dongen, B. E., Alling, V., Kosmach, D, Charkin, A., Semiletov, I.P., Dudarev, O.V., and others. Nature. 489: 137-140.

Wakeham, S. G., and Lee, C. 1993. Production, transport and alteration of particulate organic matter in the marine water column. M.A. Engle and S.A. Macko (Eds.), Organic Geochemistry: Principles and Applications. Plenum, New York, NY, 145-169.

Wang, W. X., Griscom, S. B., and Fisher, N. S. 1997. Bioavailability of Cr (III) and Cr (VI) to

marine mussels from solute and particulate pathways. Environ. Sci. Technol. 31, 603-611.

Wang, W. X., and Guo, L. 2000. Influences of natural colloids on metal bioavailability to two marine bivalves. *Environ Sci. Technol., 34*(21), 4571-4576.

Wang, Z., Liu, W., Zhao, N., Li, H, Zhang, Y., Si-Ma, W., Liu, J. 2007. Composition analysis of colored dissolved organic matter in Taihu Lake based on three dimension excitation-emission fluorescence matrix and PARAFAC model, and the potential application in water quality monitoring. J. Environ. Sci. 19: 787–791.

Waples, J. T., and Klump, J. V. 2002. Biophysical effects of a decadal shift in summer wind direction over the Laurentian Great Lakes. Geophys. Res. Lett. 29: 1–4.

Whitman, R. L., Shively, D. A., Pawlik, H., Nevers, M. B., and Byappanahalli, M. N. 2003. Occurrence of *Escherichia coli* and Enterococci in *Cladophora* (Chlorophyta) in nearshore water and beach sand of Lake Michigan. Appl. Environ. Microb. 69: 4714-4719.

Williamson, C. E., Hargreaves, B. R., Orr, P. S., Lovera, P. A. 1999. Does UV play a role in changes in predation and zooplankton community structure in acidified lakes? Limnol. Oceanogr. 44: 774–783.

Wisconsin Department of Natural Resources. 2012. Total maximum daily load and watershed management plan for total phosphorus and total suspended solids in the Lower Fox River basin and lower Green Bay.

Xu, H., Cai, H., Yu, G. and Jiang, H. 2013. Insights into extracellular polymeric substances of cyanobacterium Microcystis aeruginosa using fractionation procedure and parallel factor analysis. *Water Res. 47*(6): 2005-2014.

Yamashita, Y., Jaffé, R., Maie, N., Tanoue, E. 2008. Assessing the dynamics of dissolved organic matter (DOM) in coastal environments by excitation emission matrix fluorescence and parallel factor analysis (EEM-PARAFAC). Limnol. Oceanogr. 53: 1900–1908.

Zhang, Y., van Dijk, M. A., Liu, M., Zhu, G., Qin, B. 2009. The contribution of phytoplankton degradation to chromophoric dissolved organic matter (CDOM) in eutrophic shallow lakes: Field and experimental evidence. Water Res. 43: 4685–4697.

Zhou, Z., and Guo, L. 2012. Evolution of the optical properties of seawater influenced by the Deepwater Horizon oil spill in the Gulf of Mexico. Environ. Res. Lett, 7: 1-12

Zhou, Z., L. Guo, A. M Shiller, S. E. Lohrenz, V. L. Asper, and C. L. Osburn. 2013. Characterization of oil components from the Deepwater Horizon oil spill in the Gulf of Mexico using fluorescence EEM and PARAFAC techniques. Mar. Chem. 148: 10-21. (submitted).

Zhou, Z., Guo, L. and Minor, E. 2016. Characterization of chromophoric dissolved organic

matter in the Laurentian Great Lakes. J. Greart Lakes Res. (accepted after revision).

Zigah, P. K., Minor, E. C., and Werne, J. P. 2012. Radiocarbon and stable isotope geochemistry of organic and inorganic carbon in Lake Superior. Global Biogeochem. Cy. 26. GB1023, doi:10.1029/2011GB004132.

5. Appendices

Appendix A. Sampling locations and their hydrographic parameters, including water depth, water temperature (Temp), specific conductivity (Sp. Cond), dissolved oxygen (DO), and chlorophyll-a (Chl-*a*) in surface waters of Green Bay during June and August 2014.

Station ID	Latitude (N)	Longitude (W)	Temp (°C)	Sp. Cond ($\mu S\ cm^{-1}$)	DO ($mg\ L^{-1}$)	Chl-*a* ($\mu g\ L^{-1}$)	Water Depth (m)
			June 2014				
DePere Dam	-	-	-	-	-	-	6.7
Fox Mouth	44°32'15.72''	88°00'08.28''	22.1	410	7.25	-	7.8
GB-6	44°39'26.81''	87°53'00.74''	18.3	330	11.04	5.4	5.9
GB-12 (Sta-F)	44°45'28.20''	87°45'03.00''	18.8	327	10.11	3.3	9.9
Sta-B	44°47'15.55''	87°47'32.49''	16.9	302	10.57	2.2	11.6
GB-38 B	44°57'58.21''	87°23'48.83''	18.9	305	-	-	19.4
GB-17	44°47'37.11''	87°45'36.74''	16.5	295	10.56	2.0	13.2
GB-42	45°01'14.83''	87°22'58.99''	18.7	301	11.23	3.1	30.7
GB-20 (Sta-G)	44°50'26.64''	87°41'39.00''	17.9	298	10.14	3.2	15.3
Sta-D	44°40'18.25''	87°52'40.04''	17.6	309	10.35	1.9	6.5
GB-25 (Sta-H)	44°54'25.66''	87°32'04.37''	18.3	308	10.57	4.4	23.0
GB-30	44°55'39.98''	87°26'40.98''	17.3	298	10.72	3.7	18.0
Sta-C	44°43'42.95''	87°51'13.39''	16.9	324	10.35	-	8.8
Sta-A	44°49'48.72''	87°40'51.95''	18.1	307	10.02	1.9	14.0
GB-9 (Sta-E)	44°42'22.03''	87°49'11.65''	15.9	298	10.56	2.4	8.1
GB-26	44°53'01.22''	87°37'57.88''	14.0	293	11.32	2.1	21.4
Condos	44°56'30.28''	87°50'09.26''	12.1	300	11.14	1.2	10.2
GB-SB	44°53'42.32''	87°24'50.33''	17.3	309	-	-	13.0
GB-CI	45°10'01.60''	87°16'56.14''	14.9	300	11.07	-	18.6
GB-39	44°58'39.76''	87°30'40.16''	12.4	295	12.07	-	27.5
GB-47	45°04'00.24''	87°23'00.26''	13.8	296	12.45	3.5	29.7
GB-44 (Sta-I)	45°01'32.44''	87°28'41.06''	12.7	287	12.00	2.5	32.8
GB-64 B	45°14'21.47''	87°19'26.94''	14.6	295	11.38	-	11.3
GB-52	45°06'37.96''	87°23'02.65''	13.2	286	11.70	1.8	25.1
GB-59 (Sta-J)	45°10'17.77''	87°26'48.71''	14.0	290	10.56	1.3	29.9
GB-67	45°11'58.05''	87°26'50.67''	13.7	296	11.81	1.7	29.3
GB-48	45°04'16.12''	87°26'47.12''	12.2	281	12.40	2.3	31.2
GB-64B (Sta K)	45°12'00.91''	87°15'27.76''	14.7	-	-	-	23.8
GB-53	45°06'39.47''	87°26'42.43''	12.3	284	12.31	1.1	30.0
GB-73	45°14'38.36''	87°23'02.61	11.1	289	13.60	1.9	31.2
			August 2014				
Fox River	44°32'15.72''	88°00'08.28''	-	-	-	-	-
GB-6E	44°39'27.53''	87°49'49.44''	22.1	318	10.8	3.9	4.6
GB-SC	44°34'29.03''	87°59'06.75''	23.4	361	14.2	5.6	7.6
GB-2E	44°36'14.58''	87°56'05.11''	22.8	332	5.6	6.1	4.3
GB-2S	44°36'10.51''	87°56'49.88''	22.2	340	11.4	3.7	5.0
GB-2W	44°35'57.63''	87°57'56.29''	-	-	-	-	3.3
GB-5	44°39'27.53''	87°49'49.44''	22.6	311	7.1	5.3	6.2
GB-8	44°42'25.68''	87°45'28.09''	21.9	322	10.4	3.2	7.3
GB-1B	44°38'31.81''	87°53'17.70''	22.9	316	6.5	6.6	5.3
GB-9	44°42'19.91''	87°49'05.62''	21.9	315	12.1	3.2	8.2
GB-10B	44°41'32.09''	87°50'20.96''	22.0	312	11.2	3.7	7.5
GB-13	44°45'02.52''	87°48'28.75''	21.7	314	11.0	3.4	-
MR-Mouth	45°05'15.34''	87°32'49.95''	22.1	336	9.3	1.2	17.2
Condos	44°46'28.25''	87°50'09.79''	21.9	308	12.8	2.4	10.1

Appendix A Cont.

Station ID	Latitude (N)	Longitude (W)	Temp (°C)	Sp. Cond (µS cm^{-1})	DO (mg L^{-1})	Chl-*a* (µg L^{-1})	Water Depth (m)
August 2014 cont.							
GB-18	44°47’40.25’’	87°49’14.56’’	22.4	340	9.6	2.7	11.2
GB-30B	44°54’59.19’’	87°27’28.51’’	20.7	-	9.1	-	-
GB-12	44°44’58.52’’	87°45’49.63’’	21.6	309	11.5	3.4	9.6
GB-18B	44°48’26.76’’	87°48’06.56’’	22.3	340	10.0	5.4	11.1
GB-7	44°39’30.29’’	87°56’46.46’’	23.4	342	9.3	2.8	4.6
GB-17	44°47’40.13’’	87°45’46.16’’	21.5	308	11.6	2.2	12.2
GB-11	44°42’11.06’’	87°56’15.27’’	23.3	339	9.3	3.3	-
GB-25	44°52’30.46’’	87°33’35.36’’	20.8	296	9.3	3.1	-
GB-20	44°50’50.68’’	87°37’51.79’’	21.3	300	9.4	2.7	14.4
GB-31	44°55’17.99’’	87°30’23.36’’	21.0	339	9.5	2.5	23.7
GB-14B	44°45’25.88’’	87°52’44.90’’	22.7	340	9.6	4.0	6.1
GB-19	44°47’24.49’’	87°52’15.44’’	23.0	330	9.6	4.0	6.1
GB-32	44°55’39.63’’	87°34’14.43’’	21.1	304	10.8	1.7	-
GB-26S	44°49’24.32’’	87°40’14.24’’	21.0	305	11.3	2.4	13.2
GB-45	45°01’21.51’’	87°34’20.81’’	21.7	337	8.7	1.5	14.8
GB-22	44°50’18.35’’	87°45’33.47’’	22.0	339	9.7	3.8	13.3
GB-39	44°58’30.38’’	87°30’27.45’’	21.3	301	11.8	1.6	27.4
GB-44	45°01’12.50’’	87°30’29.90’’	21.5	300	11.4	1.5	28.0
GB-48	45°04’02.23’’	87°26’38.18’’	22.0	335	9.5	1.8	30.7
GB-48W	45°06’14.15’’	87°31’12.02’’	22.2	318	9.4	1.4	21.0
GB-30E	44°52’58.85’’	87°24’52.17’’	22.3	339	10.5	3.8	7.1
GB-30	44°55’37.91’’	87°26’45.72’’	21.4	301	13.4	2.5	17.9
GB-39-Pump	44°58’30.39’’	87°30’27.46’’	21.3	301	11.8	1.6	27.4
GB-38	44°58’28.02’’	87°26’43.57’’	23.3	318	7.3	1.3	27.4
GB-54	45°06’40.74’’	87°30’18.73’’	22.0	334	9.5	1.7	22.5
GB-43	45°01’14.88’’	87°26’51.71’’	21.2	299	11.6	1.5	31.2
GB-47	45°04’00.81’’	87°22’59.11’’	21.3	298	11.8	1.5	29.4
GB-42	45°01’09.16’’	87°23’09.90’’	21.6	300	11.7	1.6	30.7

Appendix B. Dissolved organic carbon (DOC) and optical properties of dissolved organic matter, including absorption coefficient at 254 nm (a_{25}), specific UV absorbance at 254 nm ($SUVA_{254}$), and spectral slope at 275-295 nm ($S_{275-295}$) in Green Bay in June and August 2014.

Station ID	DOC (µM-C)	a_{254} (m^{-1})	$SUVA_{254}$ (L mg-C^{-1} m^{-1})	$S_{275-295}$ (nm^{-1})
		June 2014		
DePere Dam	561	58.4	3.77	0.0173
Fox Mouth	546	56.5	3.74	0.0173
GB-6	442	35.0	2.86	0.0202
GB-12 (Sta-F)	414	33.4	2.92	0.0213
Sta-B	396	31.7	2.90	0.0194
GB-38 B	396	33.9	3.10	0.0186
GB-17	394	32.6	2.99	0.0201
GB-42	385	34.1	3.21	0.0190
GB-20 (Sta-G)	384	31.7	2.99	0.0203
Sta-D	383	31.1	2.94	0.0199
GB-25 (Sta-H)	378	32.0	3.06	0.0191
GB-30	375	32.3	3.12	0.0190
Sta-C	375	32.7	3.15	0.0192
Sta-A	374	31.1	3.01	0.0197
GB-9 (Sta-E)	374	30.4	2.94	0.0201
GB-26	371	32.1	3.13	0.0193
Condos	360	29.1	2.93	0.0197
GB-SB	354	31.2	3.19	0.0195
GB-CI	354	29.4	3.01	0.0203
GB-39	336	27.7	2.98	0.0194
GB-47	321	25.6	2.88	0.0216
GB-44 (Sta-I)	320	27.2	3.07	0.0188
GB-64 B	310	22.1	2.58	0.0213
GB-52	309	26.2	3.06	0.0185
GB-59 (Sta-J)	304	27.9	3.33	0.0188
GB-67	291	24.5	3.05	0.0207
GB-48	291	23.6	2.94	0.0189
GB-64B (Sta K)	288	22.1	2.78	0.0203
GB-53	250	17.8	2.58	0.0214
GB-73	202	12.4	2.22	0.0222
		August 2014		
Fox River	610	59.8	3.55	0.0202
GB-6E	495	40.3	2.95	0.0237
GB-SC	488	41.5	3.08	0.0247
GB-2E	458	29.8	2.35	0.0257
GB-2S	436	37.8	3.14	0.0224
GB-2W	426	38.2	3.25	0.0215
GB-5	390	27.9	2.59	0.0220

Appendix B Cont.

Station ID	DOC (µM-C)	a_{254} (m^{-1})	$SUVA_{254}$ (L mg-C^{-1} m^{-1})	$S_{275-295}$ (nm^{-1})
August 2014 cont.				
GB-8	385	28.5	2.68	0.0212
GB-1B	365	31.0	3.08	0.0212
GB-9	358	25.7	2.59	0.0217
GB-10B	356	24.2	2.46	0.0226
GB-16B	350	26.8	2.77	0.0213
GB-13	349	24.7	2.57	0.0217
MR-Mouth	349	21.2	2.20	0.0225
Condos	345	23.8	2.49	0.0225
GB-18	344	25.9	2.73	0.0211
GB-30B	342	21.5	2.28	0.0215
GB-12	339	27.4	2.92	0.0215
GB-18B	336	23.4	2.52	0.0282
GB-7	335	26.9	2.91	0.0220
GB-17	333	24.6	2.67	0.0210
GB-11	325	24.5	2.73	0.0224
GB-25	324	21.5	2.41	0.0238
GB-20	322	25.6	2.88	0.0214
GB-31	321	18.7	2.11	0.0266
GB-14B	321	25.0	2.82	0.0226
GB-19	319	24.4	2.76	0.0228
GB-32	317	21.7	2.48	0.0226
GB-26S	316	20.9	2.40	0.0257
GB-45	313	17.9	2.08	0.0261
GB-22	312	24.5	2.84	0.0222
GB-39	312	20.8	2.41	0.0230
GB-44	311	17.6	2.05	0.0266
GB-48	311	21.4	2.49	0.0221
GB-48W	310	21.1	2.46	0.0263
GB-30E	310	21.3	2.49	0.0221
GB-30	308	22.2	2.60	0.0211
GB-39-Pump	306	20.3	2.41	0.0223
GB-38	302	16.8	2.02	0.0292
GB-54	300	18.3	2.21	0.0256
GB-43	293	19.7	2.43	0.0230
GB-47	289	16.9	2.11	0.0268
GB-42	279	17.3	2.24	0.0254

Appendix C. Fluorescence indices and fluorescent-DOM component abundance derived from PARAFAC modeling based on fluorescence excitation-emission matrices for samples collected from Green Bay during June and August 2014. FIX=fluorescence index, BIX=biological index, and HIX=humification index. C1, C2, C3 and C4 are fluorescent-DOM component-1, 2, 3, and 4, respectively.

Station ID	FIX	BIX	HIX	C1	C2	C3	C4
				(ppb-QSE)			
June 2014							
DePere Dam	1.22	0.66	2.58	9.49	6.49	3.79	4.37
Fox Mouth	1.23	0.65	2.17	8.66	6.07	3.32	4.69
GB-6	1.19	0.69	2.08	5.95	3.61	2.31	4.05
GB-12 (Sta-F)	1.17	0.67	2.39	6.10	3.60	2.43	2.86
Sta-B	1.15	0.71	2.59	3.64	3.74	1.72	2.06
GB-38 B	1.11	0.67	2.94	4.57	3.37	2.10	2.11
GB-17	1.15	0.63	1.71	5.26	3.02	2.15	3.78
GB-42	1.15	0.69	2.96	4.48	3.61	1.82	1.98
GB-20 (Sta-G)	1.16	0.65	1.76	5.42	3.19	2.27	3.98
Sta-D	1.13	0.67	2.85	4.90	3.04	2.20	2.38
GB-25 (Sta-H)	1.14	0.68	3.11	5.46	2.68	2.20	2.01
GB-30	1.15	0.64	0.93	3.07	2.18	1.31	3.95
Sta-C	1.16	0.77	2.23	3.48	4.14	1.54	2.32
Sta-A	1.14	0.69	2.79	5.62	2.81	2.36	2.81
GB-9 (Sta-E)	1.13	0.66	2.76	5.44	2.87	2.20	2.56
GB-26	1.23	0.65	2.31	5.46	2.94	2.23	2.88
Condos	1.13	0.67	3.13	4.49	2.94	2.09	2.05
GB-SB	1.12	0.67	2.71	4.91	3.12	2.28	2.62
GB-CI	1.16	0.72	2.73	3.51	3.59	1.68	1.91
GB-39	1.13	0.65	1.30	5.19	2.85	2.06	4.57
GB-47	1.14	0.65	1.47	4.41	2.20	1.81	3.22
GB-44 (Sta-I)	1.15	0.68	1.55	4.20	2.50	1.73	3.59
GB-64 B	1.14	0.69	1.09	3.64	3.74	1.72	2.06
GB-52	1.11	0.65	3.05	4.07	3.30	1.93	1.95
GB-59 (Sta-J)	1.10	0.64	2.56	3.81	2.69	1.84	2.19
GB-67	1.12	0.72	2.31	2.46	2.58	1.26	1.55
GB-48	1.13	0.70	2.76	4.02	3.10	1.78	1.89
GB-64B (Sta K)	1.12	0.70	2.97	3.26	2.90	1.53	1.57
GB-53	1.09	0.66	1.38	3.03	1.87	1.33	2.68
GB-73	1.11	0.67	2.85	1.85	1.24	0.77	0.90
August 2014							
Fox River	1.24	0.66	2.78	9.39	7.87	4.28	4.49
GB-6E	1.23	0.69	1.12	5.72	5.19	7.81	2.70
GB-SC	1.21	0.68	2.41	6.29	5.23	4.22	2.97
GB-2E	1.22	0.69	1.54	5.11	4.59	4.90	2.45
GB-2S	1.22	0.70	1.65	5.77	4.40	5.74	2.70
GB-2W	1.22	0.69	1.57	5.94	5.32	5.47	2.80
GB-5	1.18	0.73	0.97	3.47	3.28	5.78	1.67

Appendix C cont.

Station ID	FIX	BIX	HIX	C1	C2	C3	C4
					(ppb-QSE)		
			August 2014 cont.				
GB-8	1.19	0.71	1.41	3.83	3.57	4.18	1.87
GB-1B	1.16	0.74	2.00	4.02	4.16	3.56	1.99
GB-9	1.17	0.75	2.25	3.39	3.44	2.59	1.69
GB-10B	1.18	0.73	1.93	4.53	3.95	3.22	2.19
GB-16B	1.17	0.72	1.44	3.51	3.32	3.78	1.75
GB-13	1.19	0.74	1.59	4.53	3.88	4.57	2.18
MR-Mouth	1.13	0.72	0.85	2.26	1.93	3.99	1.06
Condos	1.16	0.75	1.56	3.26	3.01	3.61	1.57
GB-18	1.17	0.75	1.71	3.31	3.29	3.56	1.63
GB-30B	1.16	0.73	2.58	3.05	2.66	2.07	1.49
GB-12	1.18	0.75	2.02	3.31	3.43	3.03	1.63
GB-18B	1.19	0.75	1.29	3.41	3.22	4.00	1.65
GB-7	1.18	0.74	1.77	3.46	3.20	2.77	1.68
GB-17	1.18	0.73	2.28	3.46	3.08	2.75	1.66
GB-11	1.20	0.76	3.26	3.49	3.30	1.74	1.71
GB-25	1.16	0.72	1.14	2.94	2.68	4.03	1.43
GB-20	1.18	0.73	2.61	2.54	2.84	1.63	1.28
GB-31	1.17	0.72	1.54	3.28	3.39	3.58	1.63
GB-14B	1.18	0.73	2.35	3.48	3.17	2.42	1.65
GB-19	1.17	0.74	1.70	3.60	3.25	3.01	1.76
GB-32	1.15	0.72	1.45	3.55	3.03	3.82	1.69
GB-26S	1.18	0.75	2.45	3.55	3.40	2.63	1.79
GB-45	1.16	0.73	1.53	2.55	2.75	3.07	1.32
GB-22	1.17	0.72	1.39	3.52	3.26	3.52	1.70
GB-39	1.17	0.76	1.06	1.73	1.93	3.24	0.86
GB-44	1.14	0.74	1.64	2.71	2.73	2.83	1.37
GB-48	1.17	0.70	2.04	2.87	2.66	2.61	1.44
GB-48W	1.15	0.72	1.15	2.81	2.54	3.70	1.36
GB-30E	1.16	0.77	1.58	2.70	2.84	3.14	1.36
GB-30	1.15	0.77	1.54	2.69	3.04	3.33	1.41
GB-39-Pump	1.15	0.73	1.42	2.84	2.61	3.29	1.36
GB-38	1.15	0.72	0.67	1.56	1.40	3.75	0.73
GB-54	1.16	0.72	1.05	2.91	2.75	4.23	1.46
GB-43	1.15	0.72	0.42	0.71	0.89	2.95	0.37
GB-47	1.14	0.72	1.39	2.67	2.74	3.38	1.33
GB-42	1.13	0.73	2.10	2.40	2.56	1.95	1.23